

Electrochemically Driven Water-Oxidation Catalysis Beginning with Six Exemplary Cobalt Polyoxometalates: Is It Molecular, Homogeneous Catalysis or Electrode-Bound, Heterogeneous CoO_x Catalysis?

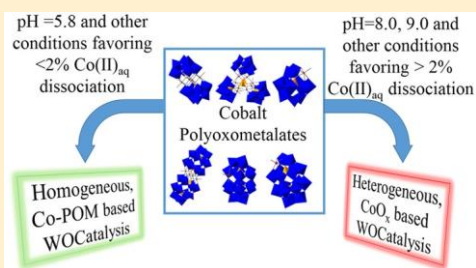
Scott J. Folkman, Joaquin Soriano-Lopez, José Ramón Galan-Mascaros, Richard G. Finke

Chemistry Department, Colorado State University, Fort Collins, Colorado 80523, United States

Institute of Chemical Research of Catalonia (ICIQ), The Barcelona Institute of Science and Technology (BIST), Av Paisos Catalans 16, E-43007 Tarragona, Spain

* Supporting Information

ABSTRACT: A series of six exemplary cobalt-polyoxometalate (Co-POM) precatalysts have been examined to determine if they are molecular water-oxidation catalysts (WOCatalysts) or if, instead, they actually form heterogeneous, electrode-bound CoO_x as the true WOCatalyst under electrochemically driven water-oxidation catalysis (WOCatalysis) conditions. Specifically, WOCatalysis derived from the following six Co-POMs has been examined at pH 5.8, 8.0, and 9.0: [Co₄(H₂O)₂(PW₉O₃₄)₂]¹⁰⁻ (Co₄P₂W₁₈), [Co₉(H₂O)₆(OH)₃(HPO₄)₂(PW₉O₃₄)₃]¹⁶⁻ (Co₉P₅W₂₇), [ββ-Co₄(H₂O)₂(P₂W₁₅O₅₆)₂]¹⁶⁻ (Co₄P₄W₃₀), [Co(H₂O)PW₁₁O₃₉]⁵⁻ (CoPW₁₁), [α₁-Co(H₂O)P₂W₁₇O₆₁]⁸⁻ (α₁-CoP₂W₁₇), and [α₂-Co(H₂O)P₂W₁₇O₆₁]⁸⁻ (α₂-CoP₂W₁₇). The amount of Co(II)_{aq} in 500 μM solutions of each Co-POM was measured after 3 h of aging as well as from t = 0 for pH = 5.8 and 8.0 by μM sensitive Co(II)_{aq}-induced ³¹P NMR line broadening and at pH = 9.0 by cathodic stripping. The amount of detectable Co(II)_{aq} after 3 h for the six Co-POMs ranges from ~0.25 to ~90% of the total cobalt initially present in the Co-POM. For 12 out of 18 total Co-POM and different pH cases, the amount Co(II)_{aq} detected after 3 h forms heterogeneous CoO_x able to account for ≥100% of the observed WOCatalysis activity. However, under 0.1 M NaPi, pH 5.8 conditions for CoPW₁₁ and α₁-CoP₂W₁₇ where ~1.5% and 0.25% Co(II)_{aq} is detectable, the measured Co(II)_{aq} cannot account for the observed WOCatalysis. The implication is that these two Co-POMs are primarily molecular, Co-POM-based, WOCatalysts under electrochemically driven, pH 5.8, phosphate-buffer conditions. Even for the single most stable Co-POM, α₁-CoP₂W₁₇, CoO_x is still an estimated ~76× faster WOCatalyst at pH = 5.8 and an estimated ~740× faster WOCatalyst at pH = 8.



INTRODUCTION

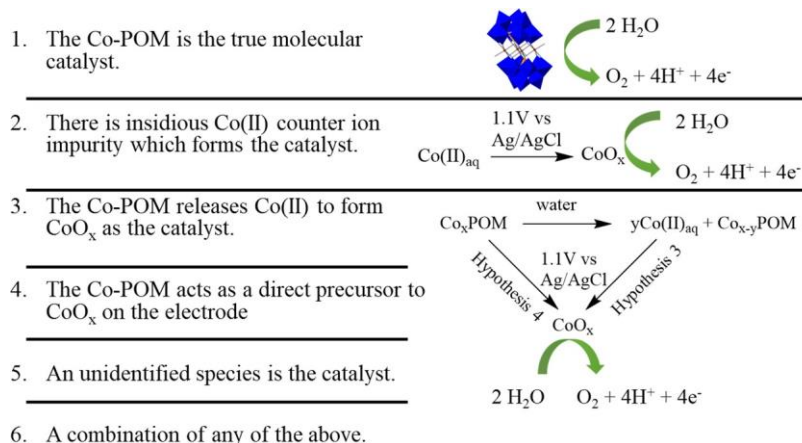
Meeting the growing global energy demand requires the development of new technologies and energy-storage schemes.^{1,2} Electrocatalytic water splitting is one widely discussed scheme for generating hydrogen as a renewable fuel.² The bottleneck of the needed electrocatalytic water splitting is the anodic half reaction, catalytic water oxidation. As such, there has been a tremendous interest in, and resultant publication on, the development and screening of water oxidation catalysts (WOCatalysts) (a SciFinder search of “water oxidation” yields 6550 hits, while “water oxidation catalysis” yields 281 references since 2000 and as of March 2018).^{3–16} The identification of the kinetically dominant WOCatalyst—the primary focus of the present study—is directly relevant to the rational development of selective, active, and long-lived WOCatalysts.

Polyoxometalates (POMs), in particular, cobalt-based polyoxometalates (Co-POMs), have attracted huge interest in the WOCatalysis area^{6,7,9–17} since Hill and co-workers initial report focussing on Co-POMs.⁹ POMs are discrete

metal oxide compounds that can be readily synthesized on the gram to kilogram or larger scale via self-assembly. POMs are typically composed of high-valent (and therefore oxidatively stable) elements such as W(VI), P(V), Mo(VI), and V(V). Interest in POMs for WOCatalysis comes from the fact that POMs are known to incorporate redox-active metal centers such as cobalt and ruthenium, both of which are active toward WOCatalysis.^{18–20}

However, no known Co-POM is 100% hydrolytically stable over a wide range of pH values. The few Co-POMs that have had their Co(II) binding constants measured show that those Co(II) binding constants are in the micromolar range.^{21,22} The micromolar amount of Co(II)_{aq} that is leached when the Co-POMs are aged in buffered solutions can then deposit onto anodes during controlled potential WOCatalysis, in turn creating a well-known heterogeneous CoO_x film⁸ as the active, electrochemically driven WOCatalyst. Such CoO_x films have

Scheme 1. List of Six Alternative Hypotheses for the Kinetically Dominant WOCatalyst under a Specific Set of Conditions



been shown to account quantitatively for all of the observed electrocatalytically driven WOCatalysis current in the case of $[\text{Co}_4(\text{H}_2\text{O})_2(\text{PW}_9\text{O}_{34})_2]^{10-}$ ($\text{Co}_4\text{P}_2\text{W}_{18}$) in 0.1 M sodium phosphate pH = 8.0 buffer and also for $[\text{Co}_4(\text{H}_2\text{O})_2(\text{VW}_9\text{O}_{34})_2]^{10-}$ ($\text{Co}_4\text{V}_2\text{W}_{18}$) in 0.1 M sodium phosphate pH = 8.0 and 5.8 buffers, as well as 0.1 M sodium borate pH = 9.0 buffer.^{21,23–27}

Our 2014 review entitled “Distinguishing Homogeneous from Heterogeneous Water Oxidation Catalysis When Beginning with Polyoxometalates” highlights the issues in, as well as preferred techniques for, distinguishing between homogeneous and heterogeneous WOCatalysis when beginning with POMs.²⁵ The main findings of that review include that (i) multiple complementary methods are necessary en route to determining the Co-POM speciation, stability, and ultimately the identity of the true WOCatalyst;^{17,25,27} (ii) the amount of redox active metal such as $\text{Co(II)}_{\text{aq}}$ that is leached into solution (or present as a counterion impurity, as discovered herein) needs to be determined quantitatively; (iii) one needs to perform control experiments examining authentic heterogeneous CoO_x self-assembled from $\text{Co(II)}_{\text{aq}}$ under the catalytic reaction conditions; (iv) the contribution to catalysis of heterogeneous CoO_x or other metal oxides must then be quantified; and overall, (v) the stability of each POM is dependent upon the unique POM structure, the structural metals (e.g., W, Mo), the heteroatoms (e.g., P, Si, others), the redox-active metal (e.g., Co, Ru), and the reaction conditions, notably the pH, buffer type, and buffer concentration. Additionally, the true WOCatalyst is often dependent on the method of oxidation (e.g., chemical, photochemical, or electrochemical).

Unfortunately, of the many studies using Co-POMs or other M-POMs (M = catalytically active metal) employed as water oxidation precatalysts, very few publications conduct the necessary experiments to provide compelling evidence for or against homogeneous molecular vs heterogeneous metal oxide WOCatalysis. There are important exceptions,^{7,13,17,23,27,28} that are discussed where relevant in the sections that follow. Other studies that use POMs for WOCatalysis, but which are not specifically treated in the main text of the present contribution, are summarized for the interested reader in Table S1 of the [Supporting Information](#). In short, if and when Co-POMs can serve as molecular WOCatalysts has remained controversial.

$[\text{Co}_4(\text{H}_2\text{O})_2(\text{PW}_9\text{O}_{34})_2]^{10-}$: A Prototype Co-POM WOCatalyst. The early prototype of a Co-POM WOCatalysis

precatalyst system is $[\text{Co}_4(\text{H}_2\text{O})_2(\text{PW}_9\text{O}_{34})_2]^{10-}$ ($\text{Co}_4\text{P}_2\text{W}_{18}$) in 0.1 M sodium phosphate pH = 8.0.^{9,23,24} Previous work has shown that, after 3 h of aging in 0.1 M NaPi solution, 500 μM $[\text{Co}_4(\text{H}_2\text{O})_2(\text{PW}_9\text{O}_{34})_2]^{10-}$ dissociates a mere 58 μM Co(II) corresponding to just 4.3% decomposition (assuming the loss of a single Co(II) from the parent Co-POM).²³ That 58 μM $\text{Co(II)}_{\text{aq}}$ forms a highly catalytically active heterogeneous CoO_x films on tin-doped indium oxide (ITO) or glassy carbon electrodes under constant potential electrolysis.²³ The resultant CoO_x film accounts for $100 \pm 12\%$ of the WOCatalysis current under the 0.1 M NaPi buffer and electrochemically driven WOCatalysis conditions.²³

However, and in experiments designed to deliberately favor molecular WOCatalysis by $\text{Co}_4\text{P}_2\text{W}_{18}$, when 2.5 μM $[\text{Co}_4(\text{H}_2\text{O})_2(\text{PW}_9\text{O}_{34})_2]^{10-}$ is dissolved in NaPi pH 8.0 or 5.8 with ≥ 600 mV overpotential, the detected amount of Co(II) cannot account for the observed WOCatalysis current under the stated conditions—evidence that CoO_x is not the dominant catalyst under those only modestly different conditions.²⁴ The now classic $\text{Co}_4\text{P}_2\text{W}_{18}$ system is a good example of how seemingly small changes in conditions can alter the kinetically dominant form of the Co-POM-derived WOCatalyst.

A second important example of a system where the formation of CoO_x from a Co-POM has been carefully examined is a 2012 *Inorg. Chem.* publication¹³ in which the Co-POM $[\text{Co}_9(\text{H}_2\text{O})_6(\text{OH})_3(\text{HPO}_4)_2(\text{PW}_9\text{O}_{34})_3]^{16-}$ ($\text{Co}_9\text{P}_5\text{W}_{27}$) was shown to form CoO_x under controlled potential electrolysis.¹³ Addition of bipyridine to starting solutions of $\text{Co}_9\text{P}_5\text{W}_{27}$ chelates leached $\text{Co(II)}_{\text{aq}}$ and prevents the formation of CoO_x under electrocatalytic conditions.¹³ WOCatalysis current was still observed in the presence of bipyridine, consistent with molecular $\text{Co}_9\text{P}_5\text{W}_{27}$ being a true, electrochemically driven, homogeneous WOCatalyst, albeit one with only $\sim 2\%$ of the WOCatalysis current of CoO_x formed in the absence of bipyridine.¹³ This is another, important conclusion from prior studies: when molecular WOCatalysis from Co-POMs is seen, that activity (at least to date) is often only 1/2–1/11th that of the activity of CoO_x examined under identical conditions.^{23–27}

Identifying the kinetically dominant WOCatalyst from a molecular precatalyst is often difficult,^{9,13,23–27} especially in cases where as much as >95 – 99% of the initial POM remains intact under the reaction conditions. Only the scientific method of multiple alternative hypotheses is able to provide

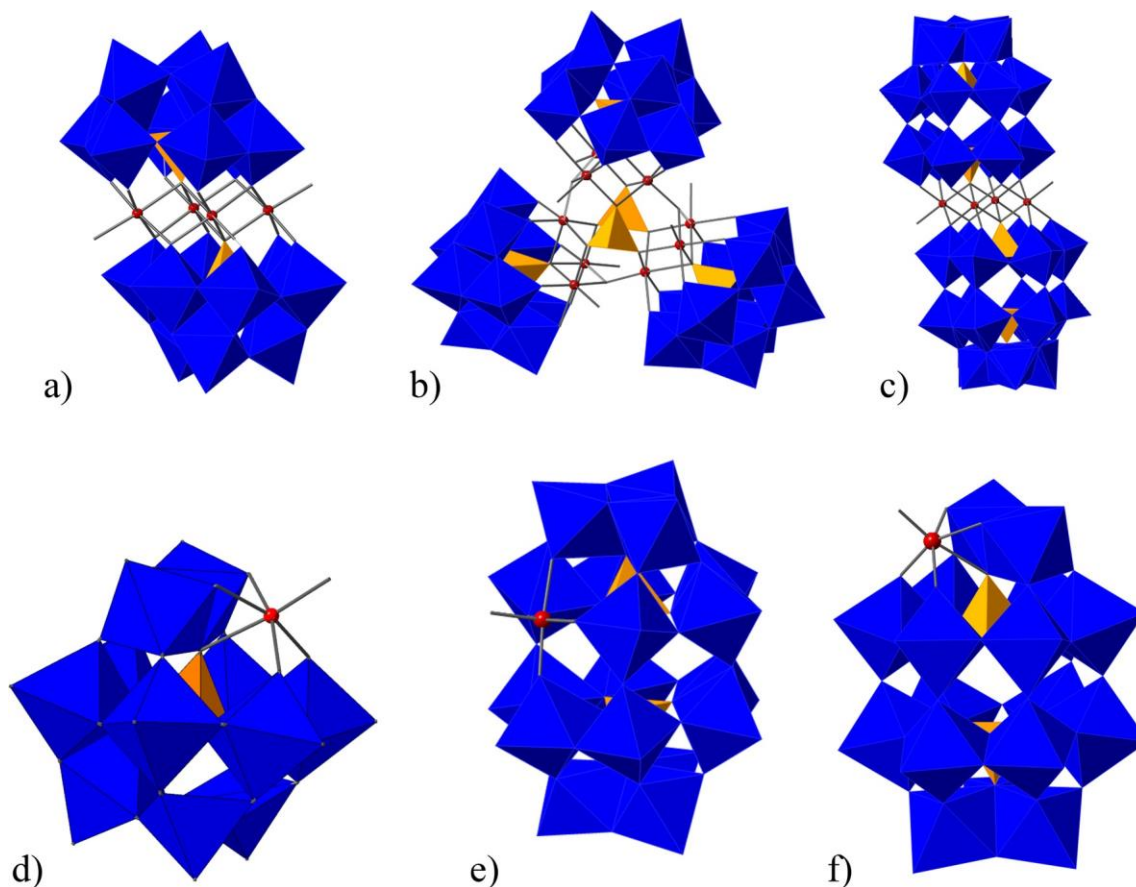


Figure 1. Polyhedral representations of the structure of the Co-POMs: (a) $\text{Co}_4\text{P}_2\text{W}_{18}$; (b) $\text{Co}_9\text{P}_5\text{W}_{27}$; (c) $\text{Co}_4\text{P}_4\text{W}_{30}$; (d) CoPW_{11} ; (e) $\alpha_1\text{-CoP}_2\text{W}_{17}$; (f) $\alpha_2\text{-CoP}_2\text{W}_{17}$. Blue octahedra represent WO_6 , orange tetrahedra represent PO_4 , and red spheres are Co(II) . The coordination site on the Co atoms typically binds H_2O and is where WOCatalysis is generally postulated to occur if the Co-POMs are indeed homogeneous, molecular WOCatalysts.

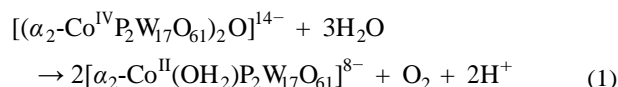
convincing, compelling evidence for the kinetically dominant, “true” WOCatalyst.^{25,29} Scheme 1 presents six alternative hypotheses for the true catalyst when beginning with molecular, M-POM precatalysts (M = metal such as Co, Ru). The first hypothesis is that the precatalyst remains intact and is a homogeneous WOCatalyst, as the evidence strongly supports for the Ru_4 -POM, $\text{Cs}_{10}[\text{Ru}_4(\mu\text{-O})_4(\mu\text{-OH})_2(\text{H}_2\text{O})_4(\text{V-SiW}_{10}\text{O}_{36})_2]$.⁷ A second hypothesis is that there is insidious Co(II) (e.g., present as a counterion from the synthesis) which then forms heterogeneous CoO_x as the dominant catalyst; Co_4O_4 cubanes being a case in point.²⁸ A third hypothesis is that the precatalyst (Co-POM) is hydrolytically unstable and leaches $\text{Co(II)}_{\text{aq}}$ into solution which then forms heterogeneous CoO_x as the WOCatalyst. Such leaching of $\text{Co(II)}_{\text{aq}}$ and then the formation of CoO_x is observed for both $\text{Co}_4\text{P}_2\text{W}_{18}$ and $\text{Co}_4\text{V}_2\text{W}_{18}$, as already noted.^{23,27} A fourth alternative hypothesis is that electrode-bound Co-POM serves as a direct precursor to CoO_x on the electrode without yielding solution-detectable $\text{Co(II)}_{\text{aq}}$. A fifth, quite reasonable hypothesis is that a fragment of the original Co-POM, POM-stabilized CoO_x nanoparticles, or perhaps some other presently unidentified species is actually the true catalyst. Lastly, it is always possible that more than one of the five hypotheses listed might be occurring simultaneously, as was the case with the formation of CoO_x from $\text{Co}_9\text{P}_5\text{W}_{27}$ where WOCatalysis activity is still observed when

$\text{Co(II)}_{\text{aq}}$ is removed by chelation with bipyridine (vide supra).¹³

Focus of the Present Studies. The focus of the current study is to establish the stability, speciation, and kinetically dominant WOCatalysts from the six exemplary Co-POMs shown in Figure 1. Three buffer and pH 5.8, 8.0, and 9.0 conditions have been selected because they are the most common buffers in the Co-POM WOCatalysis literature, and because they examine a case favoring Co-POM stability (pH = 5.8) and a case at higher pH where the thermodynamics of water oxidation are favored in the same buffer (pH = 8.0). These exemplary Co-POMs allow examination of the observed WOCatalysis as a function of varied Co(II) coordination environments (e.g., single vs multiple redox centers) and as a function of different Co(II) binding sites. The six Co-POMs chosen for study are the prototype $[\text{Co}_4(\text{H}_2\text{O})_2(\text{PW}_9\text{O}_{34})_2]^{10-}$ ($\text{Co}_4\text{P}_2\text{W}_{18}$) (because it is relatively well-studied^{9,17,23,24} and, therefore, serves as a benchmark system for controls and comparisons); $[\text{Co}_9(\text{H}_2\text{O})_6(\text{OH})_3(\text{HPO}_4)_2(\text{PW}_9\text{O}_{34})_3]^{16-}$ ($\text{Co}_9\text{P}_5\text{W}_{27}$), which has been reported to exhibit homogeneous WOCatalysis under electrocatalytically driven conditions (vide supra) and which shows very interesting, high WOCatalysis activity ($\eta = 189$ mV at 1 mA/cm²) as an insoluble Ba^{2+} salt embedded within amorphous carbon paste;^{13,30–33} and $[\beta\beta\text{-Co}_4(\text{H}_2\text{O})_2(\text{P}_2\text{W}_{15}\text{O}_{56})_2]^{16-}$ ($\text{Co}_4\text{P}_4\text{W}_{30}$), selected because its Co centers are isostructural with $\text{Co}_4\text{P}_2\text{W}_{18}$, yet this Co-POM was previously reported, surprisingly, as not exhibiting

WOCatalysis using $\text{Ru}(\text{bpy})_3^{3+}$ as the oxidant^{9,34,35} even though its close congener, $\text{Co}_4\text{P}_2\text{W}_{18}$, does.⁹ The final three of the six Co-POMs are single Co-containing $[\text{Co}(\text{H}_2\text{O})\text{-PW}_{11}\text{O}_{39}]^{5-}$ (CoPW_{11}), which has been shown to form CoO_x under electrocatalytic conditions in pH 7 phosphate buffer solutions,^{9,36–40} yet is reported to not exhibit WOCatalysis activity using $\text{Ru}(\text{bpy})_3^{3+}$ as the chemical oxidant;⁹ and $[\alpha_1\text{-Co}(\text{H}_2\text{O})\text{P}_2\text{W}_{17}\text{O}_{61}]^{8-}$ ($\alpha_1\text{-CoP}_2\text{W}_{17}$) and $[\alpha_2\text{-Co}(\text{H}_2\text{O})\text{-P}_2\text{W}_{17}\text{O}_{61}]^{8-}$ ($\alpha_2\text{-CoP}_2\text{W}_{17}$), two isomeric, single-cobalt Co-POMs^{21,22,41,42} chosen because they have literature precedent⁴³ as WOPrecatalysts and because they therefore allow insights into the role of different Co(II)-to-POM binding sites and structures on the resultant WOCatalysis and kinetically dominant WOCatalyst.

Meriting mention here is that the dicobalt(IV)- μ -oxo dimer of $\alpha_2\text{-CoP}_2\text{W}_{17}$ $[(\alpha_2\text{-Co}^{\text{IV}}\text{P}_2\text{W}_{17}\text{O}_{61})_2\text{O}]^{14-}$ (formed from $\alpha_2\text{-CoP}_2\text{W}_{17}$ using ozone as the oxidant and as an inner-sphere oxo transfer reagent) has been shown to generate O_2 from water in ~95% yield, according to eq 1.⁴⁴ However, it is not currently known if $[(\alpha_2\text{-Co}^{\text{IV}}\text{P}_2\text{W}_{17}\text{O}_{61})_2\text{O}]^{14-}$ can form from $[\alpha_2\text{-Co}^{\text{II}}(\text{H}_2\text{O})\text{P}_2\text{W}_{17}\text{O}_{61}]^{8-}$ under electrochemical oxidation. If formation of the μ -oxo dimer did occur, then one might expect to observe homogeneous WOCatalysis from $\alpha_2\text{-CoP}_2\text{W}_{17}$.



Choice of Reaction Conditions and Key Experimental Methodologies. The conditions chosen to examine the Co-POMs in Figure 1 include sodium phosphate buffer (NaPi) at both pH 5.8 (favoring the stability of the Co-POMs) and 8.0 (favoring the thermodynamics of water oxidation). We also used sodium borate buffer (NaB) at pH 9.0 to compare the effect of buffer since Co-POMs tend to be more stable in NaB buffer¹⁷ and because NaPi can, at least in principle, drive the decomposition of Co-POMs due to the formation of insoluble $\text{Co}_3(\text{PO}_4)_2$ ($K_{\text{sp}} \approx 10^{-35}$).⁴⁵ Similar to our previous publications, we aged the Co-POMs in each respective buffer for 3 h as a relatively minimal solution lifetime.^{23,27}

Note that 3 h aging is at most a minimum test of the stability of the Co-POMs because any truly useful WOCatalyst will need to be active for perhaps 10^{3-4} h or more of WOC (thereby for lifetimes that may approach an estimated $>10^9$ total turnovers),²⁷ so that even if the turnover frequency was among the highest reported for a Co-POM (i.e., 200 s^{-1}),¹⁶ then any molecular Co-POM WOCatalyst would still need to be active for >140 h—meaning that our 3 h test is only 2% of the required catalytic lifetime. However, and importantly, we also examine the amount of $\text{Co}(\text{II})_{\text{aq}}$ formation at $t \approx 0$ and as a function of time by ^{31}P NMR in what follows.

In order to quantify the amount of $\text{Co}(\text{II})$ that dissociates from the complexes, $\text{Co}(\text{II})_{\text{aq}}$ -induced ^{31}P NMR line broadening of the P atom in the phosphate buffer is used.^{27,28,46–48} Adsorptive cathodic stripping is then used in what follows as a secondary method to quantify the $\text{Co}(\text{II})_{\text{aq}}$ in NaPi and the primary method to quantify the $\text{Co}(\text{II})_{\text{aq}}$ leached from the Co-POMs in NaB.^{23,27,49} Once the stability of each Co-POM was established under a given set of conditions, controlled potential electrolysis was conducted at 1.1 V vs Ag/AgCl in the aged Co-POM solutions and the amount of O_2 produced was compared with the amount of O_2 produced from an equivalent amount of $\text{Co}(\text{II})_{\text{aq}}$ that was detected. Note that 1.1 V was chosen

because glassy carbon is known to oxidize to CO_2 at ≥ 1.2 V vs Ag/AgCl.²⁸ As such, each buffer condition has a different applied over potential of $\eta = 410$ mV at pH = 5.8, $\eta = 540$ mV at pH = 8.0, and $\eta = 600$ mV at pH = 9.0. Next, controlled potential electrolysis is conducted to allow film accumulation, followed by cyclic voltammetry in the original Co-POM solution. The electrodes were then removed and rinsed followed by cyclic voltammetry of the working electrode in a fresh, buffer-only solution, thereby obtaining the CV of any deposited film. The deposited films in what follows are also characterized by scanning electron microscopy (SEM) and X-ray photoemission spectroscopy (XPS). The sum of these experiments is then used collectively to provide evidence for the kinetically dominant WOCatalyst under a stated set of conditions.

Finally, a historical note is perhaps of some interest: we never started out to pursue the “what is the true catalyst?” question in the WOCatalysis area and despite our background with this question in the area of hydrogenation catalysis with low-valent metal nanoparticles.⁵⁰ Instead, this key question quickly found us in the area of Co-POMs as WOPrecatalysts. Our first experiments used $\text{Co}_4\text{P}_2\text{W}_{18}$ as a WOPrecatalyst in our OPV-driven WOC half-cell,⁵¹ the Co-POM $\text{Co}_4\text{P}_2\text{W}_{18}$ being “close to our intellectual hearts” since we discovered the rational synthesis of and $\text{Co}_4\text{P}_2\text{W}_{18}$, $\text{Co}_4\text{P}_4\text{W}_{30}$, and the other members of this class of M_4 -containing POMs in 1981.⁵² The very first experiments with $\text{Co}_4\text{P}_2\text{W}_{18}$ provided evidence that an electrode-bound catalyst, the same color as Nocera’s CoO_x/Pi catalyst⁸ that we had been examining, had formed on the ITO anode from the $\text{Co}_4\text{P}_2\text{W}_{18}$ precatalyst.²³ The findings quickly followed that the $\text{Co}_4\text{P}_2\text{W}_{18}$ POM leached $\text{Co}(\text{II})$ into solution from just 4.3% decomposition over 3 h, and that the resultant 58 μm $\text{Co}(\text{II})$ formed electrode-bound CoO_x that accounted for $100 \pm 12\%$ of the observed, electrochemically driven, WOCatalysis current.²³ A similar situation occurred for the V-based congener, $\text{Co}_4\text{V}_2\text{W}_{18}$: we were intrigued by the claim of 100% hydrolytic stability, and 200-fold higher catalytic activity compared to the P-congener.¹⁶ Yet when we prepared $\text{Co}_4\text{V}_2\text{W}_{18}$ by the literature route and tried to purify it to the ^{51}V NMR resonance assigned in the literature to $\text{Co}_4\text{V}_2\text{W}_{18}$, the resultant, different color POM contained only ~1 Co per $\text{V}_2\text{W}_{18}\text{O}_{68}^{18-}$ unit—yet had the same ^{51}V NMR resonance ascribed to “ $\text{Co}_4\text{V}_2\text{W}_{18}$ ”.⁵³ The 100% hydrolytic instability of $\text{Co}_4\text{V}_2\text{W}_{18}$, its decomposition to $\text{Co}(\text{II})$ and formation of electrode-bound CoO_x/Pi that carries 100% of the observed WOC within experimental error, as well as assignment of the observed ^{51}V NMR resonance to the impurity $\text{V}_2\text{W}_4\text{O}_9^{6-}$ followed after considerable effort.^{27,53} In short, the “what is the true catalyst?” question raised its omnipresent head each and every time we tried to build off the literature of Co-POMs as WO(Pre)Catalysts. That observation is, actually, not surprising, at least in hindsight: the identity of the true catalyst in any and all catalytic reactions is an important, often overlooked, typically challenging, critical question in catalysis. Reflection makes the latter claim obvious once one realizes that all catalytic properties of interest derive from the precise composition and nature of the actual catalyst, including the: catalytic activity, selectivity, lifetime, poisoning, reisolation, and catalyst regeneration. The “what is the catalyst?” question, and the associated “Is it homogeneous or heterogeneous catalysis?” question, had not been fully raised nor critically addressed for cobalt or other POM-based WOCatalysts before our 2011 study that has (as of July 2018) over 246 citations.²³ The

present work brings to completion our studies of the kinetically dominant, “true” catalyst(s) derived from exemplary Co-POMs in buffer solutions under electrochemically driven and the other stated, specific WOCatalysis conditions-conditions that matter greatly, *vide infra*. It is hoped that the WOCatalysis community can use methods and approach herein to provide evidence for the kinetically dominant WOCatalyst as a critical part of their own WOCatalysis studies.

EXPERIMENTAL SECTION

General Considerations. All reagents used were the highest purity available and were used without further purification. Water (18 M Ω) was obtained from an in house Barnstead Nanopure filtration system. FT-IR were collected using a ThermoScientific Nicolet iS50 FT-IR spectrometer in transmission mode using KBr pellets containing approximately 2 wt % of the analyte. Thermogravimetric analysis (TGA) was performed using a TA Instruments TGA 2950 with a 5 °C/min ramp rate to 500 °C on a platinum sample pan. TGA was used to determine the waters of hydration because water is the only volatile component of the Co-POMs at ≤ 500 °C. ^{31}P NMR was collected using either an Agilent (Varian) 400 MHz NMR or an Agilent Inova 500 MHz NMR; the spectral ranges and pulse sequences were optimized for the resonance of the ^{31}P atom of interest. Elemental analyses were obtained from Galbraith Laboratories in Knoxville, TN.

Electrochemically driven WOCatalysis experiments were conducted in 0.1 M sodium phosphate buffer (NaPi) either at pH 5.8 or 8.0 or in 0.1 M sodium borate (NaB) pH 9.0.⁵⁴ All stability, electrochemistry, and WOCatalysis experiments were conducted with a 500 μM Co-POM concentration, chosen because the stability of the complexes can be difficult to quantify, and hence, employing this higher, 500 μM concentration facilitates detection of decomposition byproducts by ^{31}P NMR, for example (*vide infra*).

All of the electrochemistry was performed using a CH Instruments CHI630D with a three-electrode setup. All potentials are referenced to Ag/AgCl with a platinum wire as the counter electrode and glassy carbon either 1.0 or 0.071 cm² as the working electrode. SEM was conducted on a JEOL JSM-6500F microscope with magnification from 1000 to 20000. XPS was conducted on a PE-5800 X-ray photoelectron spectrometer; full scans were collected on deposited films as well as high-resolution scans for individual elements.

Syntheses of the Co-POMs were conducted according to literature methods and characterized via FT-IR, ^{31}P NMR, TGA, and elemental analysis. The procedures followed and resulting characterization data are presented in the [Supporting Information](#) for the interested reader (Figures S1–S8).^{9,13,21,23,30,31,34–43,52} Characterization of the Co-POMs was consistent with prior literature and are isomerically pure samples, with the exception of $\text{K}_8[\alpha_1\text{-Co}(\text{H}_2\text{O})\text{P}_2\text{W}_{17}\text{O}_{61}]$, which contains a presently inseparable 5% impurity of the isomeric $\text{K}_8[\alpha_2\text{-Co}(\text{H}_2\text{O})\text{P}_2\text{W}_{17}\text{O}_{61}]$.

Stability of the Co-POMs in Buffered Solutions. Stability of the Co-POMs Determined by Co(II)-Induced ^{31}P NMR Line Broadening. The well-established method of Co(II)_{aq}-induced ^{31}P NMR line broadening of the sodium phosphate buffer, first observed by Klanberg and Dodgen⁴⁶ and used later by Nocera and others to quantify aqueous Co(II) leached out of CoO_x film or molecular Co complexes,^{27,28,47,48} was used to detect the amount of Co(II)_{aq} present in NaPi-buffered solutions for each Co-POM. This ^{31}P NMR technique is powerful because it is selective toward Co(II)_{aq} (i.e., and insensitive to Co(II) within a Co-POM) while also having a detection limit of ~ 2 μM Co(II)_{aq}.²⁶ Further precedent for this ^{31}P NMR methodology is its recent use to quantify the amount of Co(II) leached from $[\text{Co}_4\text{V}_2\text{W}_{18}\text{O}_{68}]^{10-}$ as well as $[\text{Co}_4\text{P}_2\text{W}_{18}\text{O}_{68}]^{10-}$, results which demonstrate that the ^{31}P method agrees with cathodic stripping determinations of Co(II) to within $\pm 5\%$ for both $[\text{Co}_4\text{V}_2\text{W}_{18}\text{O}_{68}]^{10-}$ and $[\text{Co}_4\text{P}_2\text{W}_{18}\text{O}_{68}]^{10-}$ in 0.1 M NaPi pH = 8.0.²⁷

We followed the same general procedure outlined in our 2017 paper²⁷ for the ^{31}P NMR determinations of Co(II)_{aq}, except the Co-POM concentrations employed herein are 500 μM . (The lower

concentration of 5 μM Co-POM used in our 2016 paper was chosen because $[\text{Co}_4\text{V}_2\text{W}_{18}\text{O}_{68}]^{10-}$ decomposes 100%, resulting in Co(II)_{aq} concentrations too high to measure reliably at more than 5 μM of that particular Co-POM). First, a calibration curve was developed using $\text{Co}(\text{NO}_3)_2$ as an authentic source of Co^{2+} _{aq} for the line broadening experiments in both pH 5.8 and 8.0 NaPi (as 100 mM solutions in 25% D₂O, Figure S9 in the [Supporting Information](#)). Next, the appropriate amount of Co-POM was weighed in a 1 dram vial. To prepare 2 mL of a 500 μM solution, 1 μmol of each POM is required; therefore the following masses of each indicated Co-POM were used: $\text{Co}_9\text{P}_5\text{W}_{27}$, 8.97 mg; $\text{Co}_4\text{P}_4\text{W}_{30}$, 8.77 mg; CoPW_{11} , 3.20 mg; $\alpha_1\text{-CoP}_2\text{W}_{17}$, 4.86 mg; $\alpha_2\text{-CoP}_2\text{W}_{17}$, 4.82 mg. Next, 1 mL of 200 mM NaPi (pH 5.8 or 8.0), 500 μL D₂O, and 500 μL water were added to the Co-POM powder in the 1 dram vial, yielding 2 mL of a solution with 500 μM Co-POM, 100 mM NaPi, and 25% D₂O. The timer was started immediately upon addition of the buffer solution to the solid Co-POM. A 1 mL aliquot was then transferred into a 5 mm OD NMR tube which was then inserted into the NMR. ^{31}P NMR was then collected on the sample without shimming and under conditions identical to those used for the calibration curve. A 500 MHz Varian NMR spectrometer was used at 25 °C with scans from +64.9 to -64.9 ppm, a 45° pulse angle, a 1.000 s relaxation delay, and a 0.624 s acquisition time. The peak width of the ^{31}P NMR peaks were determined using the instrument's VNMRJ software after phase correction.

To confirm the line broadening is caused almost completely by Co(II)_{aq} and not by the Co(II) present within the intact Co-POM, we conducted the same experiments as above except in the presence of 92 μM EDTA to complex any free Co(II) (i.e., an amount of EDTA in 1.2–10-fold excess of the Co(II)_{aq} detected by the initial ^{31}P NMR experiment for $\text{Co}_4\text{P}_4\text{W}_{30}$ and $\alpha_1\text{-CoP}_2\text{W}_{17}$ for example). Any residual line broadening over that original ^{31}P NMR was then assigned to the intact Co-POM, an amount that ranged from just 2 to 8 Hz, so only between 1.3 and 6 μM Co(II)_{aq} for $\text{Co}_4\text{P}_2\text{W}_{18}$ and $\text{Co}_4\text{P}_4\text{W}_{30}$ in 0.1 M NaPi pH = 8.0. This in turn means that the contribution from the intact Co-POMs to the observed ^{31}P NMR line broadening is at most only 8% of the Co(II)_{aq} detected for $\text{Co}_4\text{P}_4\text{W}_{30}$ in 0.1 M NaPi pH = 8.0. The residual line broadening from the added EDTA experiment was subtracted from the raw fwhm values for the particular Co-POM being examined before the fwhm values were fit to the calibration curve to calculate the final Co(II)_{aq} concentration.

For the Co(II)_{aq} values that were close to the detection limit of the initial calibration curve (e.g., $\alpha_1\text{-CoP}_2\text{W}_{17}$ at pH = 5.8 where the detected Co(II)_{aq} was 2.9 ± 3 μM) an additional calibration curve was generated that was able to more precisely determine the Co(II)_{aq} and with a lower <0.5 μM detection limit (Figure S9 of the [Supporting Information](#)).

Stability of the Co-POMs As Determined by Cathodic Adsorptive Stripping As a Second Technique. The reliability of the ^{31}P NMR technique for the quantitation of Co(II)_{aq} has been demonstrated for both $\text{Co}_4\text{P}_2\text{W}_{18}$ and $\text{Co}_4\text{V}_2\text{W}_{18}$.^{23,27} However, we wanted to determine the amount of Co(II)_{aq} present in the 500 μM Co-POM solutions in pH 9.0 NaB after 3 h of aging (i.e., and under conditions where no P_i is available for the use of the ^{31}P NMR method). Therefore, and as before,^{23,27} an adsorptive cathodic stripping method was employed that quantifies Co(II)_{aq} by adsorption of the neutral cobalt dimethylglyoxime (DMG) complex on a bismuth electrode and subsequent reductive stripping.^{23,27,49}

Electrode Preparation. The Bi film electrode was prepared using a method adapted from previous studies.^{23,27,49} First, a clean glassy carbon electrode (3 mm diameter), a Ag/AgCl reference electrode, and a Pt wire counter electrode were placed into an aqueous solution containing 0.02 M Bi(NO₃)₃, 0.5 M LiBr, and 1 M HCl. Then constant potential electrolysis was conducted at -0.25 V until 10 mC of charge had accumulated (~ 45 s). The electrodes were then removed and rinsed gently with water prior to being placed into the analyte solution containing either $\text{Co}(\text{NO}_3)_2$ for the calibration curve or the aged Co-POM solutions.

Calibration Curve. A calibration curve was developed using $\text{Co}(\text{NO}_3)_2$ as an authentic source of Co(II)_{aq}, with concentrations

ranging from 1.0 to 50 μM $\text{Co(II)}_{\text{aq}}$ in NaPi pH 8.0 and NaB pH 9.0 (Figure S10 in the Supporting Information). Using freshly plated Bi films, the electrodes were placed into a 1 dram vial containing a buffered solution (either 0.1 M NaPi pH 8.0 or 0.1 M NaB pH 9.0) that contained the desired $\text{Co(NO}_3)_2$ concentration and 100 μM DMG. The solution was stirred for 3 s and allowed to reach stillness, and then the CoDMG_2 was adsorbed by applying -1.3 V to the Bi film electrode for 15 s. The solution was again stirred for 3 s and allowed to settle before differential pulse voltammetry (DPV) from -0.7 to -1.3 V using a 0.1 s pulse width, 50 mV amplitude, and a 0.0167 s sampling width. The height of the DPV waves were measured from the background using the CH Instruments software, and plotted against the known $\text{Co(II)}_{\text{aq}}$ concentration for the calibration curves (Figure S10 in the Supporting Information). Worth noting is that the use of pH = 8.0 to 9.0 buffer is essential because at pH = 5.8 the adsorptive cathodic stripping is not responsive to the $\text{Co(II)}_{\text{aq}}$ concentration, likely because the DMG must be deprotonated by pH > 5.8 to form Co(DMG)_2 that is an intermediate in the Co-stripping on the Bi film.

Aging of the Co-POMs and Cathodic Stripping. First, 500 μM solutions of the Co-POMs were prepared by weighing an appropriate amount of the solid Co-POM material into a 1 dram vial and then adding 2 mL of either 0.1 M NaPi pH 8.0 or NaB pH 9.0. The solutions were then aged 3 h before an aliquot, typically 200 μL , was used in the same analyte solution as the calibration curve. (While as noted the aliquot was typically 200 μL , the actual microliter volume of the aliquot was adjusted such that the detected $\text{Co(II)}_{\text{aq}}$ concentration was within the calibration curve's linear range of 1–10 μM , as explained in greater detail below.) Because DMG binding of Co(II) could, in principle, shift the Co-POM dissociative equilibrium yielding a larger $\text{Co(II)}_{\text{aq}}$ concentration than without DMG, the time between aliquot addition and cathodic stripping was kept to a minimum (<1 min). The Co(DMG)_2 deposition and the DPV were conducted in the same manner as for the calibration curve above. The peak height of the DPV was fit to the calibration curves (Figure S10 of the Supporting Information), and the results were used to calculate the $\text{Co(II)}_{\text{aq}}$ concentration in the analyte solutions. The $\text{Co(II)}_{\text{aq}}$ concentration in the original solution was determined by taking into account the 1:10 dilution from the original solution to the analyte solution. For cases where the measured $\text{Co(II)}_{\text{aq}}$ was not within the linear range of the calibration curve, the dilution factor from the original to the analyte solution was adjusted so that the detected $\text{Co(II)}_{\text{aq}}$ concentration was within the range of the linear calibration curve. For example, the $\text{Co(II)}_{\text{aq}}$ detected from a 1:10 dilution of CoPW_{11} is $\gg 10$ μM and therefore outside the linear range of the calibration curve. Instead, a 20 μL aliquot of the aged CoPW_{11} was used (a 1:100 dilution) and the $\text{Co(II)}_{\text{aq}}$ concentration in the diluted solution was determined to be 4.4 ± 0.5 μM , meaning that the actual $\text{Co(II)}_{\text{aq}}$ concentration in the original, undiluted CoPW_{11} solution was 100-fold larger, specifically 440 ± 50 μM .

Electrocatalytically Driven Water Oxidation Catalysis Beginning with the Co-POMs. Electrolysis Using the Co-POMs in Buffered Solutions in Comparison with $\text{Co(II)}_{\text{aq}}$. From the ^{31}P NMR and cathodic stripping studies, the amount of $\text{Co(II)}_{\text{aq}}$ that dissociates into buffered solution after 3 h is known. Comparing the observed activity of the aged Co-POM solutions with solutions containing authentic $\text{Co(II)}_{\text{aq}}$ tests if the WOCatalysis activity can be accounted for by the dissociated $\text{Co(II)}_{\text{aq}}$ or, alternatively, if WOCatalysis by the Co-POM itself is indicated. Hence, we conducted bulk electrolysis using a 1 cm^2 working electrode in buffered solutions that either contained a 500 μM Co-POM solution that had aged 3 h or an amount of authentic $\text{Co(II)}_{\text{aq}}$ that matched the measured $\text{Co(II)}_{\text{aq}}$ after 3 h, as determined by ^{31}P NMR or cathodic stripping.

Electrolysis was conducted in the same manner as previous studies using $\text{Co}_4\text{V}_2\text{W}_{18}$ as a WOPrecatalyst.²⁷ Briefly, the experiments were conducted in a custom built U-cell with a medium fritted glass filter separating the working and counter electrodes. The working compartment was sealed using a Teflon lid pierced to accommodate the working electrode, the reference electrode, and the O_2 detection sensor (NeoFox; FOSPOR-R probe), all in a 6 mL, argon-purged

solution. The headspace was kept to a minimum in order to diminish O_2 equilibration with the headspace which otherwise results in an excessively systematically low measured O_2 concentration and low apparent faradaic efficiency. The O_2 sensor was calibrated using a 2-point calibration curve consisting of air-saturated DI water (~ 220 μM at 22 $^\circ\text{C}$, for a typical barometric pressure of 0.84 atm for Fort Collins, CO), and O_2 -free solutions were generated by addition of excess sodium sulfite to the solution. Electrolysis was conducted at 1.1 V for 5 min with stirring at ~ 600 rpm. The final faradaic efficiency was determined by comparing the final O_2 concentration to the O_2 concentration expected from the total charge passed during the experiment (i.e., $4 e^-$ passed per 1O_2 produced).

Electrochemical and Morphological Characterization of the Films Electrodeposited from the Co-POM Solutions. Deposition and Cyclic Voltammograms of CoO_x Films. Previous work has documented the value of controlled potential electrolysis and subsequent analysis of deposited films from Co-POMs.^{23,27} As such, controls were conducted in a similar manner in which constant potential electrolysis was conducted at 1.1 V on a glassy carbon electrode for 5–30 min to allow sufficient accumulation of an electrodeposited film to be visible to the naked eye. After electrolysis, cyclic voltammetry was conducted on the film in the same Co-POM solution. The electrodes were subsequently removed from the original Co-POM solution, rinsed with water, and placed into a buffer-only solution. Cyclic voltammetry was then conducted on the electrodeposited film in the buffer-only solution—this allows comparison of the observed WOCatalysis activity from the deposited film to that of the starting Co-POM solution. Electrolysis was then conducted on the deposited film in the buffer-only solution under otherwise identical conditions to the Co-POM solution.

To test the hypothesis that CoO_x forms from $\text{Co(II)}_{\text{aq}}$ and not directly from Co-POM bound to the electrode surface, EDTA was added at a concentration 10 times the measured $\text{Co(II)}_{\text{aq}}$. Constant potential electrolysis at 1.1 V was then conducted. Controls with $\text{Co(NO}_3)_2$ and EDTA present demonstrate that no film is deposited from the Co-EDTA complex. This, in turn, means that if a film is observed from any Co-POM solution containing 10 equiv of EDTA/ $\text{Co(II)}_{\text{aq}}$, then that film would have to be formed from some route not involving freely diffusing $\text{Co(II)}_{\text{aq}}$; for example, conceivably directly from Co-POM adsorbed on the electrode.

Morphological and Compositional Analysis of the Deposited Films. The electrodeposited films were examined by XPS and SEM to quantify elements in the surface of the film, and to capture morphological features, respectively. The films were deposited on glassy carbon (1 cm^2) at 1.1 V for 30 min from Co-POM solutions in 0.1 M NaPi pH 5.8 and 8.0 as well as 0.1 M NaB pH 9.0. The electrodes were then removed from solution and allowed to air-dry on the bench before being placed into a desiccator overnight. XPS was conducted on a PE-5800 X-ray photoelectron spectrometer; survey scans were collected from 10 to 1100 eV with 1.6 eV/step and 187.85 eV pass energy. High resolution scans were collected for each element detected from the survey (such that sufficient background was included with 0.1 eV/step and 23.5 eV pass energy). SEM was conducted on a JEOL JSM 6500F scanning electron microscope. Images were collected from 1000 \times to 20000 \times magnification to demonstrate the homogeneity of the film as well as to visualize morphological details.

RESULTS AND DISCUSSION

Stability of the Co-POMs Assayed by $\text{Co(II)}_{\text{aq}}$ -Induced ^{31}P NMR Line Broadening. Quantitative knowledge of the stability of any precatalyst under a given set of conditions is crucial to understanding the kinetically dominant, most active form of the catalyst.^{23,25–27} Using the $\text{Co(II)}_{\text{aq}}$ -induced, ^{31}P NMR line-broadening experiments first developed by Klanberg and Dodgen⁴⁶ and then Nocera and co-workers,^{28,47} the amount of $\text{Co(II)}_{\text{aq}}$ present as a function of time for each Co-POM was measured in NaPi pH 5.8 and 8.0. The $\text{Co(II)}_{\text{aq}}$ vs time traces for selected Co-POMs are shown in Figure 2 and

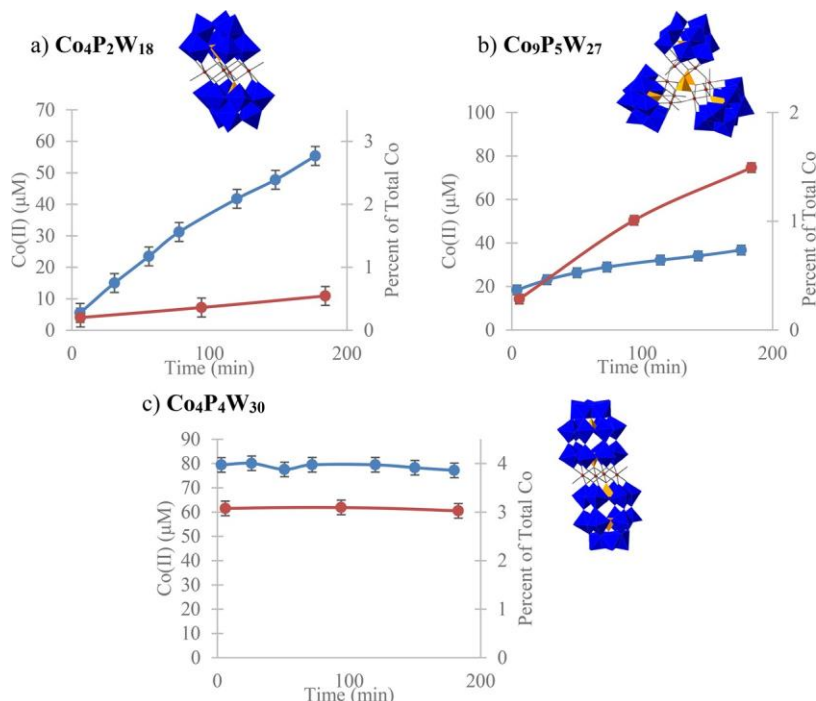


Figure 2. $\text{Co(II)}_{\text{aq}}$ concentration vs time determined by $\text{Co(II)}_{\text{aq}}$ induced line broadening in 0.1 M NaPi (pH 5.8, red and pH 8.0, blue) for 500 μM solutions of (a) $\text{Co}_4\text{P}_2\text{W}_{18}$ (adapted with permission from ref 27, Copyright 2017 American Chemical Society); (b) $\text{Co}_9\text{P}_5\text{W}_{27}$; and (c) $\text{Co}_4\text{P}_4\text{W}_{30}$. The value for each $\text{Co(II)}_{\text{aq}}$ concentration was determined by fitting the observed ^{31}P NMR line widths of the NaPi to the calibration curve generated with authentic $\text{Co(NO}_3)_2$. The percent of total cobalt refers to the percent of cobalt that is detected in solution compared to the total Co(II) present initially in the specific Co-POM. Error bars are the standard deviation from three repeat experiments. The lines between points have been added to guide the eye and, hence, are not fits to any specific equation. The $\text{Co(II)}_{\text{aq}}$ vs time plots for the other Co-POMs are shown in Figure S11 of the Supporting Information.

Figure S11 of the Supporting Information. The percent of total Co(II) in the Co-POM solution that is present as aqueous $\text{Co(II)}_{\text{aq}}$ after 3 h of aging is presented in Figure 3 and Table 1. All of the Co-POMs examined showed some detectable $\text{Co(II)}_{\text{aq}}$ over 3 h in NaPi buffer ranging from ~ 0.25 to 50% (in NaPi buffer) of the total Co(II) present in the given Co-POM solution, the exact percentage depending on the Co-POM and the precise pH and buffering conditions, vide infra.

Three of the Co-POMs examined, specifically $\text{Co}_4\text{P}_2\text{W}_{18}$, $\text{Co}_9\text{P}_5\text{W}_{27}$, and CoPW_{11} , show increasing concentration of Co(II) leached into solution over 3 h at pH = 8.0 and 5.8, Figure 2 and Figure S11 of the Supporting Information. For these cases, the detected, increasing $\text{Co(II)}_{\text{aq}}$ is most simply attributed to (continued) dissociation of Co(II) from the Co-POM precatalyst. One interesting point to note is that while $\text{Co}_4\text{P}_2\text{W}_{18}$ is more stable at pH = 5.8, $\text{Co}_9\text{P}_5\text{W}_{27}$ is more stable at pH = 8.0. This is consistent with the fact that a mixture of $\text{Co}_4\text{P}_2\text{W}_{18}$ and $\text{Co}_9\text{P}_5\text{W}_{27}$ is obtained from reactions of HPO_4^{2-} , Co(II) , and WO_4^{2-} ,³⁰ with $\text{Co}_9\text{P}_5\text{W}_{27}$ being more prevalent at the more basic pH > 7.³¹ Restated, this evidence suggests unsurprisingly that individual Co-POMs tend to be more stable in the pH range where they are synthesized. Leaching of $\text{Co(II)}_{\text{aq}}$ from the complex is consistent with hypothesis #3 from Scheme 1 for the above three Co-POMs.

The other three Co-POMs, $\text{Co}_4\text{P}_4\text{W}_{30}$, $\alpha_1\text{-CoP}_2\text{W}_{17}$, and $\alpha_2\text{-CoP}_2\text{W}_{17}$, show detectable, $0.25(\pm 0.06)$ – $3.9(\pm 0.1)\%$ but relatively flat $\text{Co(II)}_{\text{aq}}$ over 3 h at pH 5.8 and 8.0 (with the exception of $\alpha_2\text{-CoP}_2\text{W}_{17}$ at pH 8.0, vide infra). Note that all of the Co-POMs have non-zero amounts of $\text{Co(II)}_{\text{aq}}$ detected that are well above the detection limit ($\sim 2 \mu\text{M}$ generally, but $\sim 0.5 \mu\text{M}$ for $\alpha_1\text{-CoP}_2\text{W}_{17}$ at pH = 5.8 using our third, more

precise, lowest $[\text{Co(II)}_{\text{aq}}]$ calibration curve described in the Experimental section and Figure S9 of the Supporting Information, which focuses on the lower concentrations of 0.5, 1, 5, and 20 μM $\text{Co(II)}_{\text{aq}}$). Three repetitions of each of these lower $[\text{Co(II)}_{\text{aq}}]$ were conducted using $\alpha_1\text{-CoP}_2\text{W}_{17}$ at pH = 5.8, with the key result that the detected amount of $\text{Co(II)}_{\text{aq}}$ for $\alpha_1\text{-CoP}_2\text{W}_{17}$ at pH = 5.8 is $1.2 \pm 0.3 \mu\text{M}$. In short, the detected $\text{Co(II)}_{\text{aq}}$ for $\alpha_1\text{-CoP}_2\text{W}_{17}$ at pH = 5.8 is also experimentally non-zero, as well as relatively flat.

A flat $\text{Co(II)}_{\text{aq}}$ vs time dependence implies either: (i) that rapid $\text{Co(II)}_{\text{aq}}$ dissociation from the Co-POM to reach equilibrium quickly has occurred, or (ii) that the $\text{Co(II)}_{\text{aq}}$ is present as a counteranion to the Co-POM from the synthesis (or, conceivably (iii) a combination of (i) and (ii)). If the $\text{Co(II)}_{\text{aq}}$ is, in fact, present as a counteranion, then one might expect to observe a high Co(II) weight percent (wt %) in the elemental analysis.

As a specific example, the weight percent of Co by elemental analysis for $\text{Na}_{16}[\beta\beta\text{-Co}_4(\text{H}_2\text{O})_2(\text{P}_2\text{W}_{15}\text{O}_{56})_2]\cdot 39\text{H}_2\text{O}$ ($\text{Co}_4\text{P}_4\text{W}_{30}$) is the same within experimental error, with a found Co wt % of 2.62% vs the expected 2.69%. Furthermore, the molar amount of Co(II) present in the $\text{Co}_4\text{P}_4\text{W}_{30}$ solutions (14–16 mol of Co(II) /mol Co-POM) is not distinguishable if one assumes an error of ± 0.4 absolute wt %. Indeed, the expected wt % cobalt would change from 2.69% for the elemental formula of the pure $\text{Na}_{16}\beta\beta\text{-}[\text{Co}_4(\text{H}_2\text{O})_2(\text{P}_2\text{W}_{15}\text{O}_{56})]\cdot 39\text{H}_2\text{O}$ to 2.81% for the hypothetical case where 16 mol % of Co(II) / $\text{Co}_4\text{P}_4\text{W}_{30}$ as a counteranion was present for a (hypothetical) elemental formula of $\text{Na}_{15.68}\text{Co}_{0.16}[\beta\beta\text{-Co}_4(\text{H}_2\text{O})_2(\text{P}_2\text{W}_{15}\text{O}_{56})_2]\cdot 39\text{H}_2\text{O}$, a difference of only 0.11 wt %. In short, a publishable ($\pm 0.4\%$

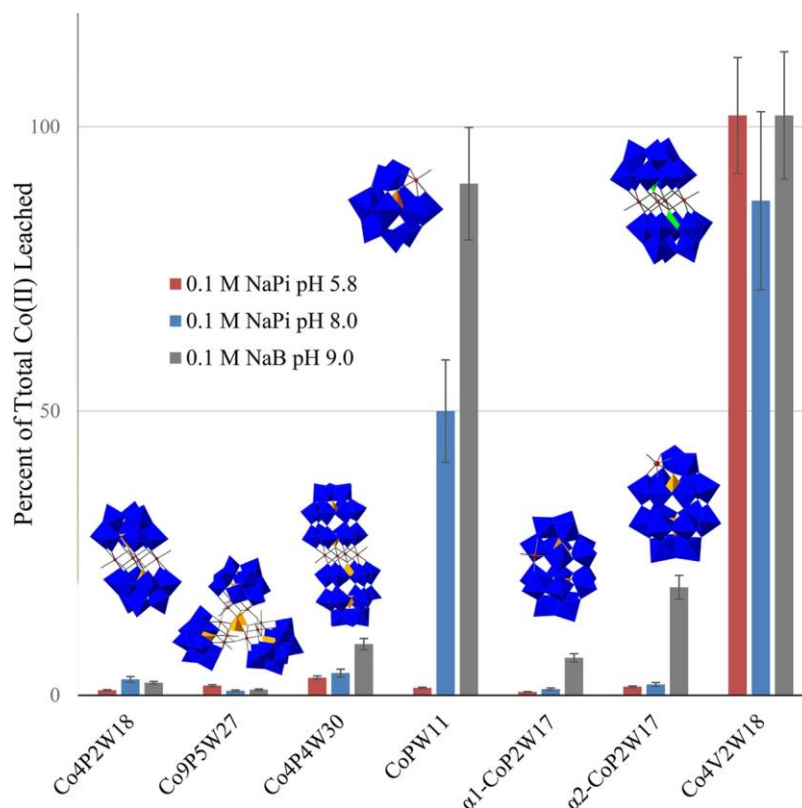


Figure 3. Percent of total cobalt that is present as $\text{Co(II)}_{\text{aq}}$ after 3 h of aging in solution for 500 μM solutions of each Co-POM in 0.1 M NaPi, pH = 5.8 (red) and pH = 8.0 (blue), as well as in 0.1 M NaB pH = 9.0 (gray). Decomposition data for $\text{Co}_4\text{V}_2\text{W}_{18}$ has been adapted with permission from ref 26 (Copyright 2017 American Chemical Society) for comparison with the other Co-POMs, albeit with a 5 μM Co-POM concentration under otherwise identical conditions. The lower concentration of $\text{Co}_4\text{V}_2\text{W}_{18}$ had to be used because $\text{Co}_4\text{V}_2\text{W}_{18}$ is so unstable that, at 500 μM , the $\text{Co(II)}_{\text{aq}}$ detected is otherwise above the linear range of the calibration curve.

absolute wt %) elemental analysis is not sufficient evidence to disprove Co(II) impurities as counter cations present in $\text{Co}_4\text{P}_4\text{W}_{30}$ nor, by analogy, more generally in other Co-POMs.

To provide evidence for or against $\text{Co(II)}_{\text{aq}}$ being present as a counterion vs the rapid dissociation of Co(II) from $\text{Co}_4\text{P}_4\text{W}_{30}$ to an equilibrium value, we conducted ^{31}P NMR control experiments by adding 1 equiv of EDTA/ $\text{Co(II)}_{\text{aq}}$ to the $\text{Co}_4\text{P}_4\text{W}_{30}$ solutions and, then, repeated the ^{31}P NMR line-broadening experiment, Figure 4. The results of that experiment show that addition of 1 equiv of EDTA/ $\text{Co(II)}_{\text{aq}}$ lowers-but does not remove all-of the detected $\text{Co(II)}_{\text{aq}}$ (black dashed line, Figure 4). Furthermore, an important observation is that the $\text{Co(II)}_{\text{aq}}$ concentration does not immediately return to the higher, 60–80 μM value, thereby ostensibly ruling out a fast, initial release of $\text{Co(II)}_{\text{aq}}$ to reach an equilibrium level at either pH of 8.0 or 5.8. Addition of an excess, 100 μM amount of EDTA does remove all of the observed $\text{Co(II)}_{\text{aq}}$, which then remains at zero and hence constant within experimental error over the 3 h experiment (black solid line, Figure 4). In short, the data suggest that the $\text{Co(II)}_{\text{aq}}$ being detected is present initially at a counterion attached tightly to the highly negatively charged, $[\beta\beta\text{-Co}_4(\text{H}_2\text{O})_2(\text{P}_2\text{W}_{15}\text{O}_{56})_2]^{16-}$ polyoxopolyanion and, therefore, not available to contribute to the phosphate line broadening to any great extent. Such tight-ion pairing between a dicationic Co(II)^{2+} and the 16 minus POM, $[\beta\beta\text{-Co}_4(\text{H}_2\text{O})_2(\text{P}_2\text{W}_{15}\text{O}_{56})_2]^{16-}$, even in water is not unreasonable nor unexpected.

The evidence provided above demonstrates that there is an EDTA-removable amount of additional ^{31}P NMR line broadening in the $\text{Co}_4\text{P}_4\text{W}_{30}$ system, consistent with an additional amount of tight ion paired Co(II) attached to the $[\beta\beta\text{-Co}_4(\text{H}_2\text{O})_2(\text{P}_2\text{W}_{15}\text{O}_{56})_2]^{16-}$. It is therefore reasonable to sum the observed $\text{Co(II)}_{\text{aq}}$ in the absence of EDTA with the observed $\text{Co(II)}_{\text{aq}}$ seen upon the addition of 1 equiv of EDTA to give the total apparent $\text{Co(II)}_{\text{aq}}$ as shown in Figure 4. Specifically, one can calculate that in pH = 5.8 buffer, the total $\text{Co(II)}_{\text{aq}}$ value = $62(\pm 1) + 19(\pm 2) = 81(\pm 2)$ μM (i.e., the solid red line plus the dashed black line yields the dashed red line in Figure 4), while in pH = 8.0 the total $\text{Co(II)}_{\text{aq}} = 78(\pm 2) + 10(\pm 3) = 88(\pm 4)$ (i.e., the solid blue line plus the dashed black line yields the dashed blue line in Figure 4). Averaging the pH 5.8 and 8.0 data yields a $\text{Co(II)}_{\text{aq}}$ value of $85(\pm 4)$ μM as an estimate of the amount of $\text{Co(II)}_{\text{aq}}$ present as a counterion from the synthesis in $\text{Co}_4\text{P}_4\text{W}_{30}$. The systematic difference of the measured $\text{Co(II)}_{\text{aq}}$ in pH 5.8 vs 8.0 of $62(\pm 1)$ vs $78(\pm 2)$ μM , respectively, is discussed in the Supporting Information for the interested reader.

The observation of Co(II) as a counterion is an important finding for at least two reasons, the first of which is because it provides evidence for hypothesis #2 from Scheme 1, where Co(II) is present as a normally undetected impurity in the postsynthesis $\text{Co}_4\text{P}_4\text{W}_{30}$.²⁸ Second, the results in Figure 4 are significant as they imply that the presence of dication impurities in the syntheses of highly charged POMs is very likely a little recognized, but more general, phenomenon in polyoxometalate and other polyanionic self-assembly syntheses.

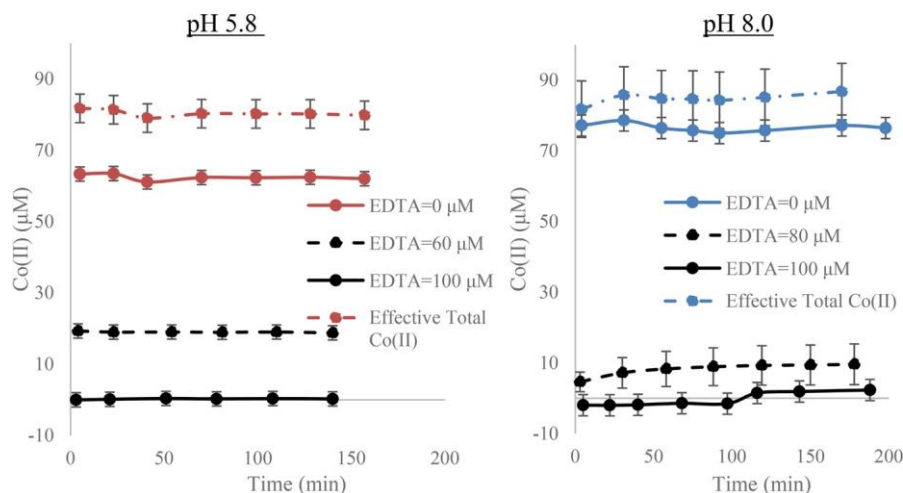


Figure 4. Plots of $\text{Co(II)}_{\text{aq}}$ concentration vs time for a 500 μM solution of $\text{Co}_4\text{P}_4\text{W}_{30}$ in 0.1 M NaPi (pH 5.8, left and pH 8.0, right). The red and blue lines are for $\text{Co}_4\text{P}_4\text{W}_{30}$ in the absence of any added EDTA (i.e., the same as Figure 2), the dashed black lines are for experiments where 1 equiv of EDTA/ $\text{Co(II)}_{\text{aq}}$ has been added (60 and 80 μM for pH 5.8 and 8.0, respectively), and solid black lines represent the addition of excess EDTA (100 μM). The dashed red and blue lines represent the true $\text{Co(II)}_{\text{aq}}$ concentration (i.e., the sum of the solid colored line with the dashed black line for each pH condition).

Because of the intrinsically high molecular weight of large POM anions, low levels of counteranion impurities are difficult to detect via standard elemental analysis methods such as ICP-OES (vide supra). This highlights the power of the $\text{Co(II)}_{\text{aq}}$ -induced ^{31}P NMR line-broadening technique because it has high selectivity toward $\text{Co(II)}_{\text{aq}}$ with a detection limit of $\sim 2 \mu\text{M}$ $\text{Co(II)}_{\text{aq}}$, which in turn corresponds to ~ 0.4 mol % regardless of the molar mass of the Co-POM. Future research using Co-POMs for WOCatalysis should use ^{31}P NMR line broadening to quantify $\text{Co(II)}_{\text{aq}}$ because it is likely present in at least some as-synthesized Co-POMs. However, the $\text{Co(II)}_{\text{aq}}$ -induced ^{31}P NMR methods herein can now be used on Co-POMs that are, for example, not run down ion-exchange columns or not exposed to multiple recrystallizations from, say, Na^+ , K^+ , or other desired cation-containing recrystallization solutions.

^{31}P NMR Line-Broadening Data for the Relatively Stable Co-POMs, $\alpha_1\text{-CoP}_2\text{W}_{17}$, and $\alpha_2\text{-CoP}_2\text{W}_{17}$. For the case of $\alpha_1\text{-CoP}_2\text{W}_{17}$ and $\alpha_2\text{-CoP}_2\text{W}_{17}$ at pH = 5.8 and 8.0 and because these Co-POMs appear to be relatively “stable” in initial $\text{Co(II)}_{\text{aq}}$ detection experiments, we conducted ^{31}P NMR experiments over a longer time scale, 7–10 h, Figure S12 of the Supporting Information. These longer time scale experiments show that at pH = 5.8 little change in the $\text{Co(II)}_{\text{aq}}$ beyond experimental error is observed. Addition of excess EDTA (92 μM) to $\alpha_1\text{-CoP}_2\text{W}_{17}$ and $\alpha_2\text{-CoP}_2\text{W}_{17}$ at pH = 5.8 returns the ^{31}P NMR line width of NaPi to its natural width of ~ 2 Hz. Overall, the results teach that $\alpha_1\text{-CoP}_2\text{W}_{17}$ and $\alpha_2\text{-CoP}_2\text{W}_{17}$ contain from $\sim 0.25\%$ to $\sim 1.5\%$ of their Co(II) in solution, a level of Co(II) that could readily be explained by either a low level of Co(II) counteranion impurity or Co(II) leaching (or a combination of these two). The bottom line is clear, however: detecting Co(II) that leads to CoO_x or other possible catalyst species derived from the parent Co-POM is a $\leq \mu\text{M}$ detection problem.

As for the pH = 8.0 experiments, observing the $\text{Co(II)}_{\text{aq}}$ concentration from $\alpha_1\text{-CoP}_2\text{W}_{17}$ over longer time-scales (10 h) at pH = 8.0 demonstrates that the $\text{Co(II)}_{\text{aq}}$ concentration increases at a slow rate without plateauing—even after 10 h. This indicates that $\alpha_1\text{-CoP}_2\text{W}_{17}$ is unstable at pH = 8.0 and

dissociating $\text{Co(II)}_{\text{aq}}$, Figure S12. Intriguingly, the $\text{Co(II)}_{\text{aq}}$ concentration from $\alpha_2\text{-CoP}_2\text{W}_{17}$ actually decreases over time in the pH 8.0 solution (Figures S11 and S12 of the Supporting Information). Possible explanations for this interesting observation, notably the possible consumption of Co(II) by the conceivable formation of $\text{Co}_4\text{P}_4\text{W}_{30}$, are discussed in the Supporting Information for the interested reader.^{55,56}

To summarize the $\text{Co(II)}_{\text{aq}}$ -induced ^{31}P NMR line-broadening experiments, all of the Co-POMs examined show nonzero detectable amounts of $\text{Co(II)}_{\text{aq}}$ under the buffer conditions specified. The amount of $\text{Co(II)}_{\text{aq}}$ released into solution ranges from $\sim 0.25\%$ to 50% of the total cobalt in 0.1 M NaPi pH = 5.8 and 8.0. Furthermore, due to the large molecular mass of the Co-POMs, cobalt elemental analysis is insufficient to quantify Co(II) present as a counteranion and at the low levels that can matter for WOCatalysis by electrode bound and formed CoO_x . However, $\text{Co(II)}_{\text{aq}}$ -induced line broadening of the ^{31}P NMR peak of NaPi is a much more useful, powerful, and relatively direct technique to quantify the amount of $\text{Co(II)}_{\text{aq}}$ either leached into solution, or present initially as a Co(II) counterion impurity from syntheses employing Co(II) .

Stability of the Co-POMs-cathodic Stripping. Because ^{11}B is a quadrupolar nucleus with relative receptivity of 0.165 compared to ^1H , and perhaps also because borate buffer has a complex speciation (especially near its pK_a , with at least 5 boron species being present),⁵⁴ $\text{Co(II)}_{\text{aq}}$ -induced ^{11}B NMR line broadening is unknown at present. Hence, to measure the amount of $\text{Co(II)}_{\text{aq}}$ that leaches from the Co-POMs after 3 h of aging in 0.1 M NaB pH 9.0 buffer, cathodic stripping was employed as the most convenient, sensitive, and selective method presently available for the NaB buffer systems.

The results of the cathodic stripping studies are summarized in Figure 3 and Table 1. The amount of $\text{Co(II)}_{\text{aq}}$ detected for the six prototype Co-POMs by ^{31}P NMR at pH 5.8 and 8.0 are also summarized in Table 1 for comparison. The amount of $\text{Co(II)}_{\text{aq}}$ detected by cathodic stripping for the 0.1 M NaPi pH = 8.0 conditions proved to be the same within experimental error to the $\text{Co(II)}_{\text{aq}}$ detected by ^{31}P NMR (the error bars are much larger for cathodic stripping, that method often

Table 1. Comparison of the Leached Co(II)_{aq} (μM) after 3 h of Solution Aging from 500 μM Co-POM Solutions under the Three Buffer Conditions (Values Shown in Bold in Parentheses are the Percent of Cobalt That Has Dissociated from the Co-POM Compared to the Total Cobalt Present Initially in the Co-POM)^a

	[Co(II) _{aq}] by ³¹ P NMR, μM (% Co(II) after 3 h)		[Co(II) _{aq}] by cathodic stripping, μM (% Co(II) after 3 h)
	0.1 M NaPi pH 5.8 [data range]	0.1 M NaPi pH 8.0 [data range]	0.1 M NaB pH 9.0 [data range]
polyoxometalate			
Co ₄ P ₂ W ₁₈	11 ± 3 (0.5 ± 0.2%) [8–15]	55 ± 3 (2.8 ± 0.3%) [52–58]	44 ± 5 (2.2 ± 0.3%) [38–49]
Co ₉ P ₅ W ₂₇	75 ± 2 (1.7 ± 0.1%) [73–77]	37 ± 2 (0.8 ± 0.1%) [35–39]	44 ± 5 (1.0 ± 0.1%) [39–50]
Co ₄ P ₄ W ₃₀	62 ± 3 (3.1 ± 0.4%) [59–66]	79 ± 3 (3.9 ± 0.1%) [77–82]	170 ± 20 (9 ± 1%) [150–192]
CoPW ₁₁	6 ± 3 (1.3 ± 0.6%) [3–9]	247 ± 3 (50 ± 5%) [245–250]	440 ± 50 (90 ± 10%) [390–490]
α ₁ -CoP ₂ W ₁₇	1.2 ± 0.3 (0.25 ± 0.06%) ^b [0.8–1.4] ^b	6 ± 3 (1.2 ± 0.6%) [3–9]	33 ± 5 (6.6 ± 0.6%) [29–38]
α ₂ -CoP ₂ W ₁₇	7.7 ± 3 (1.5 ± 0.6%) [4–11]	10 ± 3 (1.9 ± 0.6%) [7–12]	97 ± 9 (19 ± 2%) [88–106]

^aThe Co(II)_{aq} values in 0.1 M NaPi at pH 5.8 and 8.0 were determined using Co(II)_{aq}-induced line broadening ³¹P NMR. The Co(II)_{aq} values in 0.1 M NaB pH 9.0 were determined using cathodic stripping. ^bValues obtained for α₁-CoP₂W₁₇ are with the third, more precise, lower concentration Co(II)_{aq} calibration curve described in the Experimental Section, a calibration curve designed and conducted specifically for this lowest detected Co(II)_{aq} value.

complicated by W reduction waves in the differential pulse voltammetry).

The results in Table 1 further demonstrate that all of the Co-POMs show some detectable Co(II)_{aq} under any of the conditions examined, ranging from ~0.25% to now ~90% of the total cobalt present initially in the Co-POMs in the more basic, pH = 9.0 solution. Additionally, clear solution pH-dependent trends are apparent for each Co-POM, Table 1. For example, after 3 h the relatively stable CoPW₁₁ dissociates just 1.3(±0.6)% of its Co(II) in pH 5.8, but dissociates 50(±5) and 90(±10)% of its Co(II) in pH 8.0 and 9.0 solution, respectively. The pH stability of CoPW₁₁ makes sense considering that the synthesis of CoPW₁₁ relies on the partial degradation of the parent PW₁₂O₄₀³⁻ Keggin ion at pH ~ 5³⁸ (the parent PW₁₂O₄₀³⁻ itself being prepared using concentrated HCl³⁶). Hence, CoPW₁₁ is more stable at the mildly acidic pH 5.8 NaPi buffer employed and then is as expected to be less stable at the higher pH 8–9 values.

Overall, our results reiterate an undeniable fact about Co-POMs, namely that Co-POM precatalysts cannot be generally described as 100% “stable” over time under a variety of common buffer and aqueous,²⁵ WOCatalysis and pH conditions, at least as judged by whether or not Co(II)_{aq} is detectable at the ~0.25% or higher, μM level. Instead, each of Co₄P₂W₁₈, Co₉P₅W₂₇, Co₄P₄W₃₀, CoPW₁₁, α₁-CoP₂W₁₇, and α₂-CoP₂W₁₇ show somewhere between the limits seen of ~0.25–~50% detectable Co(II)_{aq} in 0.1 M, NaPi pH = 5.8

or 8.0 and up to ~90% Co(II) leaching in NaB pH = 9.0 buffer solutions. The percentage of the WOCatalysis observed that can, therefore, be attributed to CoO_x formed from even those trace levels of Co(II)_{aq} has to be carefully examined to answer the question of if the observed WOCatalysis is by the intact, molecular Co-POM or the often low-level amount of, however, high activity CoO_x formed by even trace levels of Co(II)_{aq}.

WOCatalysis Activity: Confirming the Anodic Current Is Due to Water Oxidation. To ensure that the anodic current being observed is from water oxidation, and not some other process such as oxidation of the glassy carbon electrode (which has been observed in potentials greater than +1.4 V vs Ag/AgCl),²⁸ we quantified the O₂ produced under standard conditions of 500 μM Co-POM aged 3 h or Co(NO₃)₂ (6–500 μM), 0.1 M NaPi pH = 5.8 or 8.0, and NaB pH = 9.0 and at 1.1 V vs Ag/AgCl for 5 min. The theoretical O₂ yield for each electrolysis experiment was calculated by dividing the total charge passed in coulombs (determined by integrating the current over time) by the charge of an electron (1.602 × 10⁻¹⁹ C/e⁻) and using the stoichiometry of 4 e⁻ passed per each 1O₂ produced. The O₂ concentration was monitored using an Ocean Optics NEOFOX O₂-detection probe. By dividing the measured O₂ yield at the end of the reaction by the theoretical O₂ yield, the Faradaic efficiency of the reaction was also determined.

The observed Faradaic efficiency ranged from 80 to 100% in all cases. Additionally, a ca. 8% decline in the detected O₂ concentration over a ~ 1 min period after the electrolysis is stopped is almost surely due to O₂ equilibration with the reaction vessel’s (minimized) headspace or possibly some escape from the electrochemical cell. In short, the Faradaic efficiency of O₂ production is at least ≥80–100%, and because of this, the anodic current can be used as a semiquantitative metric to compare WOCatalysis activity of the Co-POMs and authentic CoO_x (i.e., and to within a ± < 20% error), more than sufficient for any of the conclusions reached in the present work.

WOCatalysis Activity: O₂ Evolution from Co-POMs in Comparison with the Amount of Co(II)_{aq} Released. Constant potential electrolysis was conducted on 3 h aged 500 μM solutions of the Co-POMs and Co(NO₃)₂ in each of the buffer conditions. The Co(NO₃)₂ concentrations chosen to compare with each Co-POM were based upon the amount of Co(II)_{aq} that was detected in each buffer condition, Table 1, vide supra. The O₂ produced by each Co-POM is summarized in Table S2 of the Supporting Information. The amount of WOCatalysis activity that can be attributed to Co(II)_{aq} is shown in Table 2, in which the O₂ yield from Co(II)_{aq} is divided by the O₂ yield from the Co-POM (eq 2). A value of 100% (or more) means that all of the catalysis can quantitatively accounted for by Co(II)_{aq}. For example, the percentage of WOCatalysis activity that can be attributed to Co(II)_{aq} for Co₄P₂W₁₈ in NaPi pH = 8.0 is 150 ± 50%. Such values near or >100% mean that the Co(II)_{aq} present is able to account for all of the WOCatalysis under those specific conditions.

$$\begin{aligned} & \% \text{ of WOCatalysis contributable to Co(II)}_{\text{aq}} \\ &= \frac{\text{O}_2 \text{ yield from Co(II)}_{\text{aq}}}{\text{O}_2 \text{ yield from Co-POM}} \times 100 \end{aligned} \quad (2)$$

Values significantly above 100% (e.g., for α₂-CoP₂W₁₇ at pH 9.0, 800 ± 300%, Table 2) indicate that the equivalent amount

Table 2. Percent of WOCatalysis Activity That Can Be Accounted for by $\text{Co(II)}_{\text{aq}}$ for the Co-POMs under Each Buffer Condition^a

polyoxometalate	buffer system		
	0.1 M NaPi pH 5.8	0.1 M NaPi pH 8.0	0.1 M NaB pH 9.0
$\text{Co}_4\text{P}_2\text{W}_{18}$	60 ± 30%	150 ± 50%	400 ± 200%
$\text{Co}_9\text{P}_3\text{W}_{27}$	70 ± 60%	96 ± 24	300 ± 200%
$\text{Co}_4\text{P}_4\text{W}_{30}$	60 ± 40%	140 ± 70%	140 ± 70%
CoPW_{11}	20 ± 20%	180 ± 40%	100 ± 40%
$\alpha_1\text{-CoP}_2\text{W}_{17}$	16 ± 6% ^b	90 ± 30%	350 ± 40%
$\alpha_2\text{-CoP}_2\text{W}_{17}$	60 ± 60%	90 ± 50%	800 ± 300%

^aThe Co-POMs (500 μM) were aged for 3 h under each buffer condition. Electrolysis was then conducted at 1.1 V vs Ag/AgCl. The O_2 yield (μmol) was determined as described in the text and is listed in Table S2 of the Supporting Information. To compare with the amount of $\text{Co(II)}_{\text{aq}}$ that is leached, $\text{Co(NO}_3)_2$ was used in the concentrations determined and the amounts are summarized in Table 1. The amount of O_2 produced from the $\text{Co(II)}_{\text{aq}}$ was divided by the amount of O_2 produced from the Co-POMs to determine the percent of WOCatalysis activity that can be accounted for by the $\text{Co(II)}_{\text{aq}}$ present. ^bData obtained using the third, lower $\text{Co(II)}_{\text{aq}}$ calibration curve described in the Experimental Section and designed specifically for the $\alpha_1\text{-CoP}_2\text{W}_{17}$ POM system.

of $\text{Co(II)}_{\text{aq}}$ that is detected after 3 h has a greater WOCatalysis activity than the films generated from Co-POMs. The $\gg 100\%$ values are interesting, and suggest several possible interpretations, including: (i) that the Co-POM somehow poisons CoO_x films made from $\text{Co(II)}_{\text{aq}}$ in the presence of Co-POMs (indeed, evidence of W incorporation is demonstrated in some Co-POM derived films, vide infra); (ii) that the NO_3^- somehow enhances the catalysis in CoO_x made from $\text{Co(NO}_3)_2$; (iii) that the $\text{Co(II)}_{\text{aq}}$ values determined by ³¹P NMR or cathodic stripping are somewhat higher than the true $\text{Co(II)}_{\text{aq}}$ values; or possibly (iv) that the film formation (and, for example, the surface area and number of active sites) is affected by the pH⁵⁴ or the presence of POMs, which in turn affects the observed WOCatalysis. However, the most obvious, and most important, conclusion is (v) that CoO_x formed from at least $\text{Co}^{\text{II}}(\text{NO}_3)_2$ is a better WOCatalyst at pH 8 and 9 than any of the Co-POMs tested.

Values $\ll 100\%$ are also of considerable interest because they are consistent with molecular, homogeneous Co-POM WOCatalysis or conceivably consistent with some other, presently unknown, ostensibly homogeneous catalyst derived from the Co-POM (alternative hypothesis #5 from Scheme 1). However, considering that both CoPW_{11} and $\alpha_1\text{-CoP}_2\text{W}_{17}$ are stable in NaPi pH = 5.8 (decomposing by 1.3% and 0.25%, respectively, at this pH), and given that the decomposition byproduct detected is $\text{Co(II)}_{\text{aq}}$ and (by mass balance) the lacunary $\text{PW}_{11}\text{O}_{39}^{7-}$ and $[\alpha_1\text{-P}_2\text{W}_{17}\text{O}_{61}]^{10-}$ (which do not contain oxidizable metals that can serve as at least facile WOCatalysts), the simplest (Ockham's razor) interpretation of the $\ll 100\%$ data is that the intact CoPW_{11} and $\alpha_1\text{-CoP}_2\text{W}_{17}$ are the dominant WOCatalysts under those specific pH 5.8 NaPi conditions. For example, the percentage of WOCatalysis activity that can be attributed to $\text{Co(II)}_{\text{aq}}$ for CoPW_{11} and $\alpha_1\text{-CoP}_2\text{W}_{17}$ in NaPi pH = 5.8 is 20(±20)% and 16(±6%), respectively. These data, in turn, imply that intact CoPW_{11} and $\alpha_1\text{-CoP}_2\text{W}_{17}$ are the dominant electrochemically driven WOCatalyst at pH = 5.8 for 80(±20)% and 84(±6)% of the observed current. In short, the $\ll 100\%$ data in Table 2 are

consistent with if not strongly supportive of the interpretation that the most stable Co-POMs examined, CoPW_{11} and $\alpha_1\text{-CoP}_2\text{W}_{17}$, are serving as electrochemically driven, molecular WOCatalysts, a previously unavailable, important conclusion given the controversy about when and where Co-POMs can be molecular WOCatalysts.

Looking more broadly at Table 2, there are several overarching trends in the data and even given the inherently large error bars in Table 2 (that derive from having to detect mere micromolar levels of $\text{Co(II)}_{\text{aq}}$ as discussed more in the Supporting Information): at lower pH the Co-POMs account for a greater amount of the WOCatalysis. At higher pH the WOCatalysis current from $\text{Co(II)}_{\text{aq}}$ becomes increasingly prevalent, with Co(II) accounting for $\geq 100\%$ of the observed WOCatalysis activity. This pH trend in $\text{Co(II)}_{\text{aq}}$ contribution to WOCatalysis activity makes sense considering that the Co-POMs examined are often (although not always) more stable at the lower pH, for example, CoPW_{11} decomposes by only 1.3(±0.6)% at pH 5.8 but decomposes by 50(±5)% and 90(±10)% at pH 8.0 and 9.0, respectively. Hence, unsurprisingly, the Co-POMs examined are more likely to be intact WOCatalyst under conditions where they are demonstrably more stable, pH values closer to the pHs at which they form and are synthesized. Also worth noting here is that the CoO_x catalyst is also affected by pH as previously reported,⁵⁷ with CoO_x being more active at higher pH, and not being stable below pH = 3.5.⁵⁷

Greater WOCatalysis Activity of CoO_x Compared to That of the Most Stable Co-POMs. Lastly, although our evidence supports CoPW_{11} and $\alpha_1\text{-CoP}_2\text{W}_{17}$ as homogeneous WOCatalysts at pH = 5.8, a critical point is that the CoO_x formed from the equivalent amount of $\text{Co(II)}_{\text{aq}}$ is an estimated ~35–150-fold faster WOCatalyst at pH = 5.8 than is the corresponding homogeneous Co-POM (as detailed in the Supporting Information). Even using the ranges and error bars on the data in Tables 1 and 2 to bias the estimate as much as possible in favor of the Co-POM as the catalyst (and then also for the single most stable Co-POM examined, $\alpha_1\text{-CoP}_2\text{W}_{17}$) still yields the insight that CoO_x formed from the released $\text{Co(II)}_{\text{aq}}$ is at least 35-fold more active than $\alpha_1\text{-CoP}_2\text{W}_{17}$ (see the Supporting Information for details).

If one does this same calculation for, again, the most stable $\alpha_1\text{-CoP}_2\text{W}_{17}$ but now at pH = 8, the CoO_x is at least 80-fold more active if (and if one again biases the calculation as much as the data allow in favor of Co-POM-based catalysis; see the Supporting Information for details of these estimates), and likely ~740-fold more active at pH = 8 (see the Supporting Information for the detailed calculations).

To summarize, comparing the WOCatalysis activity of the 3 h aged Co-POMs with the amount of detected $\text{Co(II)}_{\text{aq}}$ reveals that at pH = 8.0 in 0.1 M NaPi and pH = 9.0 in 0.1 M NaB all of the six exemplary Co-POMs examined give rise to heterogeneous CoO_x as the dominant WOCatalyst. However, at pH = 5.8 in 0.1 M NaPi and under electrochemically driven WOCatalysis conditions, the evidence strongly suggests that CoPW_{11} and $\alpha_1\text{-CoP}_2\text{W}_{17}$, and perhaps also $\text{Co}_4\text{P}_2\text{W}_{18}$ and $\alpha_2\text{-CoP}_2\text{W}_{17}$, can serve as homogeneous, molecular WOCatalysts, albeit with CoO_x being ~35–150 \times faster at pH = 5.8 and, most likely, ~740 \times faster at pH = 8 (numbers that can be refined using the methods herein if others require greater precision than reported). One key, unequivocal conclusion from the present studies is clear, however: CoO_x is at least a ≥ 10 -fold more active WOCatalyst under electrochemical

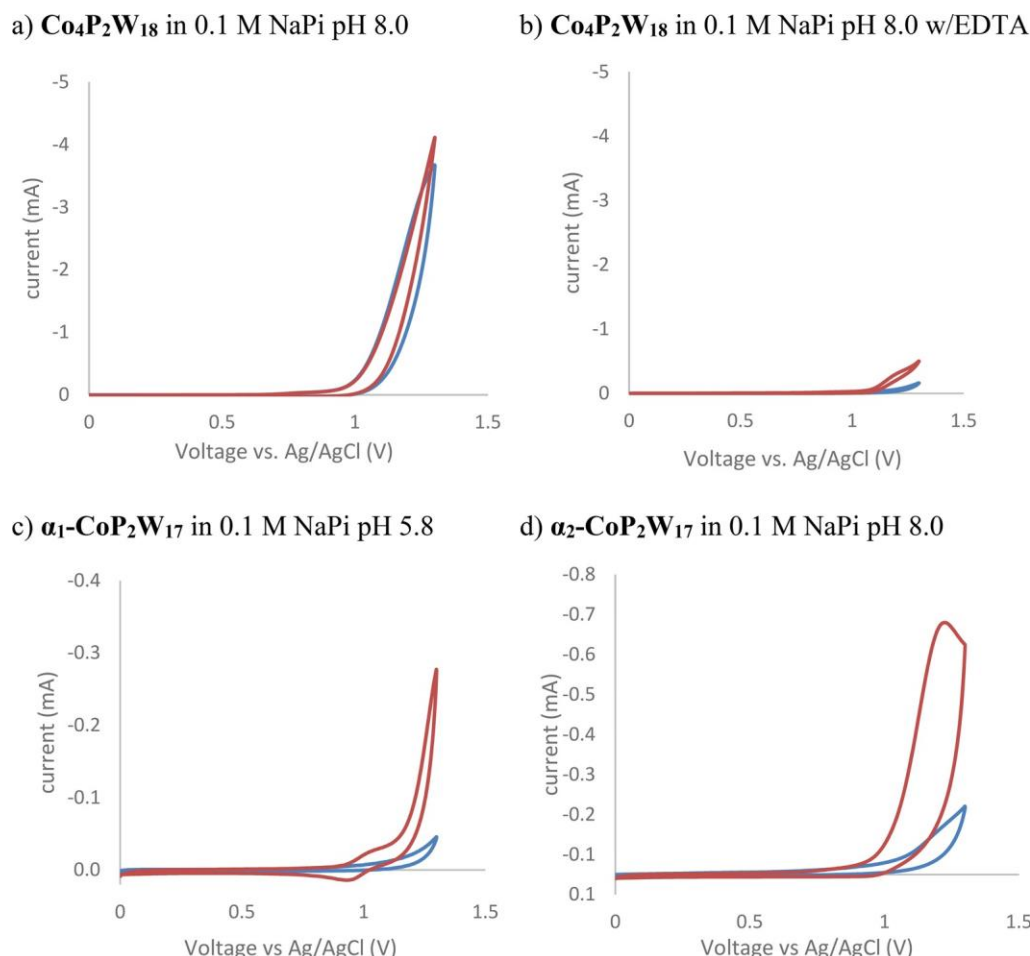


Figure 5. Selected CVs of electrodes after 5 min controlled potential electrolysis in the original Co-POM solution (red) and once the electrodes were removed, rinsed, and replaced into a fresh, buffer-only solution (blue): (a) $\text{Co}_4\text{P}_2\text{W}_{18}$ in 0.1 M NaPi pH 8.0; (b) $\text{Co}_4\text{P}_2\text{W}_{18}$ in 0.1 M NaPi pH 8.0 with $120 \mu\text{M}$ EDTA (2 equiv/ $\text{Co}(\text{II})_{\text{aq}}$); (c) $\alpha_1\text{-CoP}_2\text{W}_{17}$ in 0.1 M NaPi pH 5.8; (d) $\alpha_2\text{-CoP}_2\text{W}_{17}$ in 0.1 M NaPi pH 8.0. The remainder of the CVs are shown in the [Supporting Information](#).

conditions than any of the Co-POMs examined to date for any of the pHs (5.8, 8.0, 9.0) and buffers examined.

Electrochemical Characterization of the Deposited Films. Previous studies have shown that electrode-bound heterogeneous CoO_x formed from aged Co-POM solutions is active toward WOCatalysis.^{23,27} Additionally, such CoO_x films remain active when the working electrode is removed from the original Co-POM solution and placed in a fresh, buffer-only solution,^{23,27} thereby providing a way to characterize what amount of the WOCatalysis current detected is attributable to the film.

Controls similar to those performed before^{23,27} were therefore conducted in which controlled potential electrolysis (5–30 min) was conducted in $500 \mu\text{M}$ solutions of Co-POM that had been aged 3 h. Cyclic voltammetry (CV) was then conducted first in the original Co-POM solution. The electrodes were subsequently removed, rinsed gently with water, replaced into a fresh, buffer-only solution, and a second CV was obtained. The resultant before and after CVs for selected Co-POMs are shown in [Figure 5](#); the rest of the CVs for the Co-POMs and additional CV experiments are provided in [Figure S13 Supporting Information](#). [Figure 5a](#) is a control demonstrating that the previously reported, known^{23,24} catalytically active film from $\text{Co}_4\text{P}_2\text{W}_{18}$ can be reproducibly formed as part of the present studies from a $500 \mu\text{M}$ solution

of $\text{Co}_4\text{P}_2\text{W}_{18}$ in 0.1 M NaPi at pH 8.0 and after 3 h aging. [Figure 5b](#) is a second control that tests the possibility raised previously²⁴ (but heretofore not tested) that CoO_x might directly form from Co-POMs as well as from $\text{Co}(\text{II})_{\text{aq}}$ at sufficiently oxidizing potentials. Hence, the experiment reported in [Figure 5b](#) also contains $500 \mu\text{M}$ $\text{Co}_4\text{P}_2\text{W}_{18}$ in 0.1 M NaPi at pH 8.0 that has aged 3 h, but now has been spiked after aging with $120 \mu\text{M}$ EDTA to chelate the free $\sim 60 \mu\text{M}$ $\text{Co}(\text{II})_{\text{aq}}$ known to be formed. Almost all of the WOCatalysis activity is diminished, and no significant film is formed, implying that $\text{Co}_4\text{P}_2\text{W}_{18}$ does not serve as a direct precursor to CoO_x at pH 8.0, thereby disproving hypothesis #4 from [Scheme 1](#).

The CVs shown in [Figure 5c,d](#) present the CVs after electrolysis in the original buffer solution and then in a buffer-only solution for $\alpha_1\text{-CoP}_2\text{W}_{17}$ in 0.1 M NaPi at pH 5.8 and $\alpha_2\text{-CoP}_2\text{W}_{17}$ in 0.1 M NaPi at pH 8.0, respectively (both after 3 h of solution aging). The significantly higher current and unique CV features of the original Co-POM solution, vs those for the rinsed electrode replaced into buffer-only solution CV, provide additional evidence for a solution-based species having a role in the observed WOCatalysis for $\alpha_1\text{-CoP}_2\text{W}_{17}$, $\alpha_2\text{-CoP}_2\text{W}_{17}$, and CoPW_{11} . The Ockham's razor based hypothesis is that, under conditions where a Co-POM such as $\alpha_1\text{-CoP}_2\text{W}_{17}$ in 0.1 M NaPi at pH 5.8 is relatively stable (less than 2% detectable

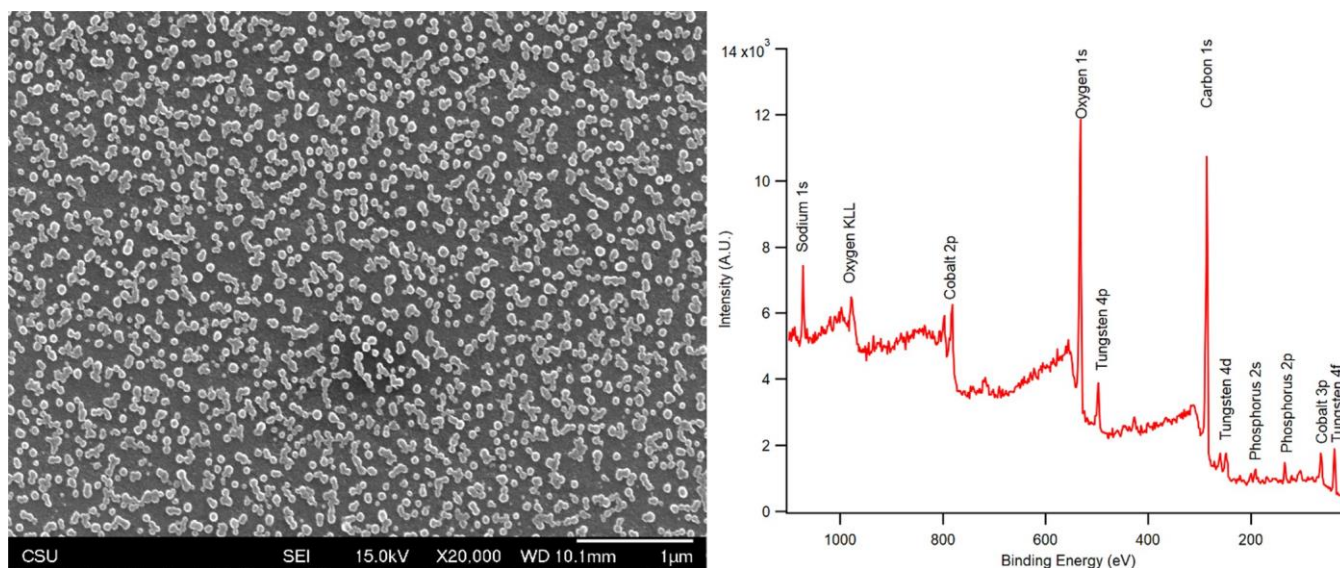


Figure 6. SEM micrograph (left) and XPS (right) of electrodes after 30 min bulk electrolysis from a 3 h aged solution of 500 μM $\alpha_2\text{-CoP}_2\text{W}_{17}$ in 0.1 M NaPi pH 8.0. The globular nature of the film is similar to previously observed films from Co(II) or Co-POMs.^{8,23,26} The *i* vs *t* curve for the film deposition is presented in Figure S14 of the Supporting Information.

Co(II)_{aq}), the $\alpha_1\text{-CoP}_2\text{W}_{17}$ is serving as a molecular, homogeneous WOCatalyst—albeit one with $\geq 10\times$ lower WOCatalysis current than the CoO_x films formed from the less stable Co-POMs (Table S2).

In summary, electrolysis and CV of the electrodes in the electrolyzed solutions (red traces in Figure 5 and Figure S13 of the Supporting Information) followed by electrolysis in buffer-only solutions (blue traces in Figure 5 and Figure S13 of the Supporting Information) helps illuminate whether the active catalyst is a solution-based species or an electrode bound species. The results are in good agreement with the percent WOCatalysis activity from the previous section. For example, at pH 5.8 the percent WOCatalysis evidence suggests that Co₄P₂W₁₈, CoPW₁₁, $\alpha_1\text{-CoP}_2\text{W}_{17}$, and $\alpha_2\text{-CoP}_2\text{W}_{17}$ can serve as molecular, homogeneous WOCatalyst. The CVs for those Co-POMs in pH 5.8 provide additional evidence in support of a solution-based WOCatalyst (Figure 5 and Figure S13 of the Supporting Information). Other Co-POMs that show evidence of a solution-based WOCatalyst in NaPi at pH = 8.0 are Co₉P₅W₂₇, $\alpha_1\text{-CoP}_2\text{W}_{17}$, and $\alpha_2\text{-CoP}_2\text{W}_{17}$, whereas in NaB pH = 9.0 only $\alpha_1\text{-CoP}_2\text{W}_{17}$ exhibits evidence of a solution-based WOCatalyst (Figure 5 and Figure S13 of the Supporting Information). Note that although at pH = 9.0 the CVs of Co₉P₅W₂₇, $\alpha_1\text{-CoP}_2\text{W}_{17}$, and $\alpha_2\text{-CoP}_2\text{W}_{17}$ at pH = 8.0 and $\alpha_1\text{-CoP}_2\text{W}_{17}$ provide evidence of a solution-based WOCatalyst, the results in Table 2 provide evidence that under those at pH = 9.0 conditions, CoO_x is still the dominant WOCatalyst.

Morphological and Compositional Characterization of Deposited Films. Most of the Co-POMs showed an increase in WOCatalysis activity for longer electrolysis times, which is characteristic of CoO_x film deposition (Figure S14 of the Supporting Information).^{8,23,27} Hence, we conducted electrolysis for 30 min to allow film accumulation and then dried the films for SEM and XPS characterization.

Figure 6 shows a typical electrode-bound film of globular particles that are formed from 3 h aged solutions of 500 μM $\alpha_2\text{-CoP}_2\text{W}_{17}$ in 0.1 M NaPi pH 8.0. The XPS of the film from $\alpha_2\text{-CoP}_2\text{W}_{17}$ contains carbon (from the glassy carbon substrate), oxygen, cobalt, sodium, phosphorus, and tungsten,

Figure 6 (right). The Co/W atom ratio from the high-resolution XPS scans was determined to be 2.1:1.3, whereas the Co/W ratio in the structure is 1:17, meaning that although W incorporation does occur, the original Co-POM is not a major component. This experiment was reproduced twice and similar XPS spectra were obtained, demonstrating reproducible W incorporation into CoO_x films produced from 500 μM $\alpha_2\text{-CoP}_2\text{W}_{17}$ in 0.1 M NaPi pH 8.0. Relevant here is that W incorporation into CoO_x films formed in the presence of aqueous Na₂WO₄ are both known and exhibit different WOC activity than seen for pure CoO_x films formed from just Co(II) in the absence of W.⁵⁸ The presence of tungsten in films formed from $\alpha_2\text{-CoP}_2\text{W}_{17}$ therefore differs from CoO_x films that form from Co₄P₂W₁₈ and Co₄V₂W₁₈ that do not contain tungsten^{23,27} and from films formed from just Co(II). In short, using Co-POMs as a precatalyst for films that make W-containing CoO_x films involves two (unintended) leached elements of the original Co-POM.

Next, 30 min electrolysis was conducted on 3 h aged solutions of 500 μM Co₄P₂W₁₈ in 0.1 M NaPi pH 8.0 with 10 equiv of EDTA/Co(II)_{aq} added after 3 h aging, but prior to electrolysis. The SEM and XPS of that particular electrode is presented in Figure 7 and confirms that heterogeneous CoO_x does not form in the presence of excess EDTA from 3 h aged solutions of 500 μM Co₄P₂W₁₈ in 0.1 M NaPi pH 8.0. This finding provides further evidence that the Co-POM cannot form CoO_x directly from, for example, putative electrode-bound Co-POM. Instead, the CoO_x film observed when starting with the Co₄P₂W₁₈ precatalyst is formed by Co₄P₂W₁₈ releasing Co(II)_{aq}, consistent with hypothesis #3 (i.e., and not #4) from Scheme 1, vide supra.

Additional CV experiments using 3 h aged 500 μM $\alpha_1\text{-CoP}_2\text{W}_{17}$ in 0.1 M NaPi pH 5.8 are discussed in the Supporting Information (Figures S15 and S16). The main results from those experiments using this more stable Co-POM is that although catalytic current increases, an electrode bound film is not formed from the bulk electrolysis of the Co-POM solution.

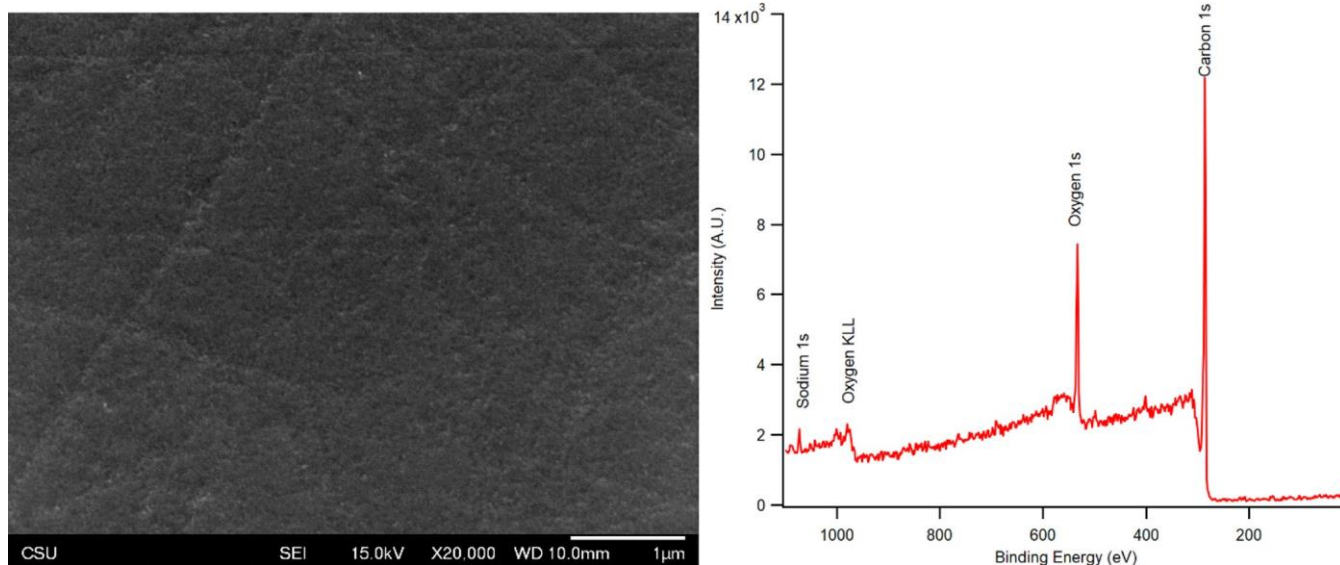


Figure 7. SEM micrograph (left) and XPS (right) of electrodes after 30 min bulk electrolysis from a 3 h aged solution of 500 μM $\text{Co}_4\text{P}_2\text{W}_{18}$ in 0.1 M NaPi pH 8.0 with 600 μM EDTA (10 equiv/ $\text{Co}(\text{II})_{\text{aq}}$). The i vs t curve for the film deposition is presented in Figure S14 of the [Supporting Information](#).

To summarize the experiments on the electrochemical and morphological characterization of the deposited films, under conditions where the Co-POMs show >2% detectable $\text{Co}(\text{II})_{\text{aq}}$, CoO_x is formed and that film accounts quantitatively for the observed WOCatalysis (Table 2, Figure 3, and Figures S13 and S16 of the [Supporting Information](#)). However, under conditions where the Co-POMs are more stable (<2% detectable $\text{Co}(\text{II})_{\text{aq}}$) such as with α_1 - $\text{CoP}_2\text{W}_{17}$, no detectable electrode-bound CoO_x is seen. Rather, a solution-based species is responsible for the observed WOCatalysis current (Table 2, Figures 5, and Figures S13 and S15 of the [Supporting Information](#)), again and ostensibly the starting Co-POM at the Ockham's razor level of interpretation. Lastly, addition of a 10-fold excess of EDTA (vs the amount of free $\text{Co}(\text{II})_{\text{aq}}$ detected) prevents the formation of CoO_x , at least with 3 h aged solution of 500 μM $\text{Co}_4\text{P}_2\text{W}_{18}$ in 0.1 M NaPi pH 8.0 (Figure 7). This, too, is evidence that CoO_x is formed from $\text{Co}(\text{II})_{\text{aq}}$ and not from intact, electrode-bound Co-POM.

SUMMARY AND CONCLUSIONS

The present study details the broadest and most quantitative, micromolar-level examination to date of the stability and electrochemically driven WOCatalysis from Co-POM precatalysts. Six exemplary Co-POMs [$\text{Co}_4(\text{H}_2\text{O})_2(\text{PW}_9\text{O}_{34})_2$] $^{10-}$ ($\text{Co}_4\text{P}_2\text{W}_{18}$), [β,β - $\text{Co}_4(\text{H}_2\text{O})_2(\text{P}_2\text{W}_{15}\text{O}_{56})_2$] $^{16-}$ ($\text{Co}_4\text{P}_4\text{W}_{30}$), [$\text{Co}_9(\text{H}_2\text{O})_6(\text{OH})_3(\text{HPO}_4)_2(\text{PW}_9\text{O}_{34})_3$] $^{16-}$ ($\text{Co}_9\text{P}_5\text{W}_{27}$), [$\text{Co}(\text{H}_2\text{O})\text{PW}_{11}\text{O}_{39}$] $^{5-}$ (CoPW_{11}), [α_1 - $\text{Co}(\text{H}_2\text{O})\text{P}_2\text{W}_{17}\text{O}_{61}$] $^{8-}$ (α_1 - $\text{CoP}_2\text{W}_{17}$), and [α_2 - $\text{Co}(\text{H}_2\text{O})\text{P}_2\text{W}_{17}\text{O}_{61}$] $^{8-}$ (α_2 - $\text{CoP}_2\text{W}_{17}$) were synthesized, their structural integrity established, and then their stability and electrochemically driven WOCatalysis examined under pH 5.8, 8.0, and 9.0 buffer conditions chosen from the literature. Importantly, the amount of $\text{Co}(\text{II})_{\text{aq}}$ leached from the Co-POMs into solution was quantified directly, at the μM -level, using $\text{Co}(\text{II})_{\text{aq}}$ -induced line broadening of the ^{31}P NMR resonance of phosphate buffer at pH 5.8 and 8.0, and by cathodic stripping in the case of pH 9.0 borate buffer. The WOCatalysis activity derived from the Co-POM precatalysts was then compared with the WOCatalysis

activity of the equivalent amount of $\text{Co}(\text{II})_{\text{aq}}$ present in solution from each of the Co-POMs.

The main conclusions from this study are the following:

- Significantly, $\text{Co}(\text{II})_{\text{aq}}$ at the micromolar or higher level was detected for every Co-POM under each set of pH and buffer conditions. The amount of detectable $\text{Co}(\text{II})_{\text{aq}}$ as a percentage of the total cobalt present in each Co-POM varies from $\sim 0.25\%$ to 50% (and up to 90% in borate buffer at pH 9) of the total $\text{Co}(\text{II})$ after 3 h in solution, the precise amount being unique to the POM structure/ $\text{Co}(\text{II})$ binding site and notably the pH and buffer, higher pH values and phosphate buffer in general leading to higher levels of $\text{Co}(\text{II})_{\text{aq}}$ (Figure 2 and Table 1, vide supra).
- In the case of Co-POMs with high anionic charge such as [β,β - $\text{Co}_4(\text{H}_2\text{O})_2(\text{P}_2\text{W}_{15}\text{O}_{56})_2$] $^{16-}$ ($\text{Co}_4\text{P}_4\text{W}_{30}$), $\text{Co}(\text{II})$ can be present as a counteranion impurity—a likely more general phenomenon for M^{n+} ions used in the synthesis of M^{n+} -POMs. While ion-exchange resin, recrystallization from counterion-controlled solutions, or other counteranion control efforts may be able to remove such counteranion impurities, that remains to be demonstrated by \leq micromolar-sensitive methods such as those employed herein.
- In 12 out of the 18 Co-POM cases at pH 8.0 and 9.0 in Table 2, the amount of heterogeneous CoO_x generated from the detected $\text{Co}(\text{II})_{\text{aq}}$ accounts for $\geq 100\%$ of the observed activity—meaning that under those higher pH conditions the kinetically dominant, electrochemically driven WOCatalyst is heterogeneous CoO_x . In those cases, using simple $\text{Co}(\text{II})$ salts to prepare the resultant, high-activity CoO_x would be a far easier, greener, and overall better use of chemicals, time, and synthetic effort.
- In terms of catalytic rate, at pH 8.0 and for the single most stable Co-POM, α_1 - $\text{CoP}_2\text{W}_{17}$, the CoO_x catalyst formed from $\text{Co}(\text{II})_{\text{aq}}$ is an estimated at least 80-fold if not ~ 740 -fold more active than any (undetectable) Co-POM based WOC. As an illustrative example, this means that (using the 740-fold value) even $\sim 0.14\%$ of

decomposition of α_1 -CoP₂W₁₇ to Co(II)_{aq} would be able in turn, at pH = 8.0, to carry $\geq 99\%$ of the catalytic WOCatalysis current. Put in other words, finding the kinetically dominant true WOCatalyst when starting with 500 mM Co-POMs is a μM detection and detective problem.

- However, under pH 5.8 conditions where the Co-POMs are generally more stable, the amount of Co(II)_{aq} detected cannot account for the observed WOCatalysis. Specifically, for CoPW₁₁ and α_1 -CoP₂W₁₇ at pH 5.8 where $\sim 1.3\%$ and $\sim 0.25\%$ detectable Co(II)_{aq} are seen, respectively, $80(\pm 20\%)$ and $84(\pm 6\%)$ of the observed WOCatalysis activity can be ascribed (in the Ockham's razor interpretation) to molecular, Co-POM-based catalysis, Table 2, vide supra. That said, the Co-POM-based WOCatalysis rate is still an estimated ~ 35 to 150 -fold slower than that for an equivalent amount of CoO_x for even the most stable Co-POM examined, α_1 -CoP₂W₁₇.
- In general, our findings confirm and fully support those of prior workers who have concluded that the reaction conditions are important in determining the identity of the kinetically dominant WOCatalyst derived from Co-POMs.^{17,24–27} We emphasize here that all of our experiments were deliberately conducted under electrochemical conditions; the nature of the true WOCatalysts under chemical or photochemical oxidation (e.g., using Ru(III)bpy₃³⁺ or Ru(II)bpy₃²⁺ + hv) will likely be different under those (different) conditions. That said, the method of multiple alternative hypotheses, particularly those listed in Scheme 1, are expected to prove useful to future researchers striving to determine experimentally the true, kinetically dominant WOCatalyst under their own oxidant, pH, buffer, and other specific conditions.
- A summary of additional POMs used in WOCatalysis which are not discussed in the main text, yet merit further study as to the identity of the true catalyst, are presented in Table S1 of the Supporting Information for the interested reader.

Finally and overall, the results obtained and presented herein in combination with prior notable work from others in the field of electrocatalytic WOCatalysis^{7,13,17,23–27} suggest that even more hydrolytically stable Co-POM and other Metal-POM WOCatalysts merit further development. The combined results also illustrate a successful, arguably preferred methodology for distinguishing molecular homogeneous from metal oxide heterogeneous WOCatalysts, even when metal-leaching or counteraction contamination is present at just micromolar levels. It is hoped that these efforts will allow even more stable and active Co-POM based WOCatalysts to be developed, studies also hopefully now able to report compelling evidence for or against molecular, Co-POM-based vs heterogeneous, CoO_x-based WOCatalysis.

ASSOCIATED CONTENT

Supporting Information

The Supporting Information is available free of charge on the ACS Publications website at DOI: 10.1021/jacs.8b06303.

Tables S1 and S2, Figures S1–S16, and a brief discussion of the error bars in Table 2 (PDF)

AUTHOR INFORMATION

Corresponding Author

*richard.finke@colostate.edu

ORCID[®]

José Ramón Galan-Mascaros: 0000-0001-7983-9762

Richard G. Finke: 0000-0002-3668-7903

Present Address

[§]Present address: School of Chemistry and CRANN/AMBER Nanoscience Institute, Trinity College, College Green, Dublin 2, Ireland.

Notes

The authors declare no competing financial interest.

ACKNOWLEDGMENTS

Funding from NSF Grant Nos. CHE-1361515 and 1664646 is gratefully acknowledged. It is also a pleasure to acknowledge discussions and cooperation with Professor Craig Hill and his research group, discussions and a cooperation which have helped highlight the issues and complexities in establishing the true catalyst in Co-POM precatalyst-based WOCatalysis. Finally, Dr. Jordan Stracke is thanked for early thoughts about this project, and for preparing the sample of Co₄P₂W₁₈ used herein.

REFERENCES

- (1) Turner, J. A. *Science* 1999, 285, 687–689.
- (2) Lewis, N. S.; Nocera, D. G. *Proc. Natl. Acad. Sci. U. S. A.* 2006, 103, 15729–15735.
- (3) Karkas, M.; Åkermark, B. *Dalton Trans* 2016, 45, 14421–14461.
- (4) Llobet, A. *Molecular Water Oxidation Catalysis*, 1 ed.; Wiley, 2014.
- (5) Liu, F.; Concepcion, J. J.; Jurss, J. W.; Cardolaccia, T.; Templeton, J. L.; Meyer, T. J. *Inorg. Chem.* 2008, 47, 1727–1752.
- (6) Geletii, Y. V.; Botar, B.; Kögler, P.; Hillesheim, D. A.; Musaev, D. G.; Hill, C. L. *Angew. Chem., Int. Ed.* 2008, 47, 3896–3899.
- (7) Sartorel, A.; Carraro, M.; Scorrano, G.; Zorzi, R. D.; Geremia, S.; McDaniel, N. D.; Bernhard, S.; Bonchio, M. *J. Am. Chem. Soc.* 2008, 130, 5006–5007.
- (8) Kanan, M. W.; Nocera, D. G. *Science* 2008, 321, 1072–1075.
- (9) Yin, Q.; Tan, J. M.; Besson, C.; Geletii, Y. V.; Musaev, D. G.; Kuznetsov, A. E.; Luo, Z.; Hardcastle, K. I.; Hill, C. L. *Science* 2010, 328, 342–345.
- (10) Huang, Z.; Luo, Z.; Geletii, Y. V.; Vickers, J. W.; Yin, Q.; Wu, D.; Hou, Y.; Ding, Y.; Song, J.; Musaev, D. G.; Hill, C. L.; Lian, T. J. *J. Am. Chem. Soc.* 2011, 133, 2068–2071.
- (11) Zhu, G.; Geletii, Y. V.; Kögler, P.; Schilder, H.; Song, J.; Lense, S.; Zhao, C.; Hardcastle, K. I.; Musaev, D. G.; Hill, C. L. *Dalton Trans* 2012, 41, 2084.
- (12) Zhu, G.; Glass, E. N.; Zhao, C.; Lv, H.; Vickers, J. W.; Geletii, Y. V.; Musaev, D. G.; Song, J.; Hill, C. L. *Dalton Trans* 2012, 41, 13043–13049.
- (13) Goberna-Ferron, S.; Vigara, L.; Soriano-Lopez, J.; Galan-Mascaros, J. R. *Inorg. Chem.* 2012, 51, 11707–11715.
- (14) Car, P.-E.; Guttentag, M.; Baldrige, K. K.; Alberto, R.; Patzke, G. R. *Green Chem.* 2012, 14, 1680.
- (15) Evangelisti, F.; Car, P.-E.; Blacque, O.; Patzke, G. R. *Catal. Sci. Technol.* 2013, 3, 3117.
- (16) Lv, H.; Song, J.; Geletii, Y. V.; Vickers, J. W.; Sumliner, J. M.; Musaev, D. G.; Kögler, P.; Zhuk, P. F.; Bacsá, J.; Zhu, G.; Hill, C. L. *J. Am. Chem. Soc.* 2014, 136, 9268–9271.
- (17) Vickers, J. W.; Lv, H.; Sumliner, J. M.; Zhu, G.; Luo, Z.; Musaev, D. G.; Geletii, Y. V.; Hill, C. L. *J. Am. Chem. Soc.* 2013, 135 (38), 14110–14118.
- (18) Pope, M. T. *Heteropoly and Isopoly Oxometalates*; Springer-Verlag, 1983.

- (19) Yamase, T.; Pope, M. *Polyoxometalate Chemistry for Nano-Composite Design*; Springer Science & Business Media, 2006.
- (20) Pope, M.; Muller, A. *Polyoxometalates: From Platonic Solids to Anti-Retroviral Activity: From Platonic Solids to Anti-Retroviral Activity*; Springer Science & Business Media, 1994.
- (21) Contant, R.; Ciabrini, J.-P. *J. Chem. Res.* 1982, 50–51.
- (22) Contant, R. *J. Chem. Res.* 1984, 120–121.
- (23) Stracke, J. J.; Finke, R. G. *J. Am. Chem. Soc.* 2011, 133, 14872–14875.
- (24) Stracke, J. J.; Finke, R. G. *ACS Catal.* 2013, 3, 1209–1219.
- (25) Stracke, J. J.; Finke, R. G. *ACS Catal.* 2014, 4, 909–933.
- (26) Stracke, J. J.; Finke, R. G. *ACS Catal.* 2014, 4 (1), 79–89.
- (27) Folkman, S. J.; Finke, R. G. *ACS Catal.* 2017, 7, 7–16.
- (28) Ullman, A. M.; Liu, Y.; Huynh, M.; Bediako, D. K.; Wang, H.; Anderson, B. L.; Powers, D. C.; Breen, J. J.; Abruna, H. D.; Nocera, D. G. *J. Am. Chem. Soc.* 2014, 136 (50), 17681–17688.
- (29) Platt, J. R. *Science* 1964, 146 (3642), 347–353.
- (30) Weakley, T. J. R. *J. Chem. Soc., Chem. Commun.* 1984, 21, 1406–1407.
- (31) Galan-Mascaros, J. R.; Gomez-Garcia, C. J.; Borrás-Almenar, J. J.; Coronado, E. *Adv. Mater.* 1994, 6 (3), 221–223.
- (32) Soriano-Lopez, J.; Goberna-Ferron, S.; Vígara, L.; Carbo, J. J.; Poblet, J. M.; Galan-Mascaros, J. R. *Inorg. Chem.* 2013, 52 (9), 4753–4755.
- (33) Blasco-Ahicart, M.; Soriano-Lopez, J.; Carbo, J. J.; Poblet, J. M.; Galan-Mascaros, J. R. *Nat. Chem.* 2018, 10 (1), 24–30.
- (34) Darenbourg, M. *Inorganic Syntheses*; John Wiley & Sons, 1998; Vol. 32, pp 175–182.
- (35) Ruhlmann, L.; Costa-Coquelard, C.; Canny, J.; Thouvenot, R. *Eur. J. Inorg. Chem.* 2007, 2007, 1493–1500.
- (36) Bailar, J. C.; Booth, H. S.; Grennert, M. *Phosphotungstic Acid*. In *Inorganic Syntheses*; Booth, H. S., Ed.; John Wiley & Sons, Inc., 1939; pp 132–133.
- (37) Weakley, T. J. R.; Malik, S. A. *J. Inorg. Nucl. Chem.* 1967, 29, 2935–2944.
- (38) Tourné, C. M.; Tourné, G. F.; Malik, S. A.; Weakley, T. J. R. *J. Inorg. Nucl. Chem.* 1970, 32, 3875–3890.
- (39) Jorris, T. L.; Kozik, M.; Casan-Pastor, N.; Domaille, P. J.; Finke, R. G.; Miller, W. K.; Baker, L. C. W. *J. Am. Chem. Soc.* 1987, 109, 7402–7408.
- (40) Li, J.; Wang, J.; Zhang, L.; Sang, X.; You, W. *J. Coord. Chem.* 2017, 70, 2950–2957.
- (41) Contant, R.; Klemperer, W. G.; Yaghi, O. *Potassium Octadecatungstodiphosphates(V) and Related Lacunary Compounds*. *Inorganic Syntheses*; Ginsberg, A. P., Ed.; John Wiley & Sons, Inc., 1990; pp 104–111.
- (42) Samonte, J. L.; Pope, M. T. *Can. J. Chem.* 2001, 79, 802–808.
- (43) Lyon, D. K.; Miller, W. K.; Novet, T.; Domaille, P. J.; Evitt, E.; Johnson, D. C.; Finke, R. G. *J. Am. Chem. Soc.* 1991, 113, 7209–7221.
- (44) Barats-Damatov, D.; Shimon, L. J. W.; Weiner, L.; Schreiber, R. E.; Jimenez-Lozano, P.; Poblet, J. M.; de Graaf, C.; Neumann, R. *Inorg. Chem.* 2014, 53 (3), 1779–1787.
- (45) Haynes, W. M.; Lide, D. R. *Handbook of Chemistry and Physics*, 92nd ed.; Taylor and Francis Group, 2011.
- (46) Klanberg, F.; Hunt, J. P.; Dodgen, H. W. *Naturwissenschaften* 1963, 50 (3), 90–91.
- (47) Surendranath, Y.; Lutterman, D. A.; Liu, Y.; Nocera, D. G. *J. Am. Chem. Soc.* 2012, 134 (14), 6326–6336.
- (48) Bazzan, I.; Volpe, A.; Dolbecq, A.; Natali, M.; Sartorel, A.; Mialane, P.; Bonchio, M. *Catal. Today* 2017, 290, 39–50.
- (49) Krolicka, A.; Bobrowski, A.; Kalcher, K.; Mocak, J.; Svancara, I.; Vytras, K. *Electroanalysis* 2003, 15 (23–24), 1859–1863.
- (50) Widegren, J. A.; Finke, R. G. *J. Mol. Catal. A: Chem.* 2003, 198 (1), 317–341.
- (51) Kirner, J. T.; Stracke, J. J.; Gregg, B. A.; Finke, R. G. *ACS Appl. Mater. Interfaces* 2014, 6 (16), 13367–13377.
- (52) Finke, R. G.; Droege, M.; Hutchinson, J. R.; Gansow, O. J. *Am. Chem. Soc.* 1981, 103 (6), 1587–1589.
- (53) Folkman, S. J.; Kirner, J. T.; Finke, R. G. *Inorg. Chem.* 2016, 55 (11), 5343–5355.
- (54) Baes, C.; Mesmer, R. *The Hydrolysis of Cations*; John Wiley & Sons, 1976.
- (55) Finke, R. G.; Droege, M. W.; Domaille, P. J. *Inorg. Chem.* 1987, 26 (23), 3886–3896.
- (56) Ruhlmann, L.; Nadjó, L.; Canny, J.; Contant, R.; Thouvenot, R. *Eur. J. Inorg. Chem.* 2002, 2002, 975–986.
- (57) Gerken, J. B.; McAlpin, J. G.; Chen, J. Y. C.; Rigsby, M. L.; Casey, W. H.; Britt, R. D.; Stahl, S. S. *J. Am. Chem. Soc.* 2011, 133 (36), 14431–14442.
- (58) Zhang, B.; Wu, X.; Li, F.; Yu, F.; Wang, Y.; Sun, L. *Chem. - Asian J.* 2015, 10, 2228–2233.